Supporting Information

Cross-Linked DNA: Site Selective "Click" Ligation in Duplexes with Bis-Azides and Stability Changes Caused by Internal Cross-Links

Hai Xiong and Frank Seela*

Laboratory of Bioorganic Chemistry and Chemical Biology, Center for Nanotechnology, Heisenbergstraße 11, 48149 Münster, Germany and Laboratorium für Organische und Bioorganische Chemie, Institut für Chemie, Universität Osnabrück, Barbarastraße 7, 49069, Osnabrück, Germany.

Corresponding author:

Phone: +49(0)251 53406 500; Fax: +49(0)251 53406 857

E-mail: Frank.Seela@uni-osnabrueck.de;

Homepage: www.seela.net

Table of contents

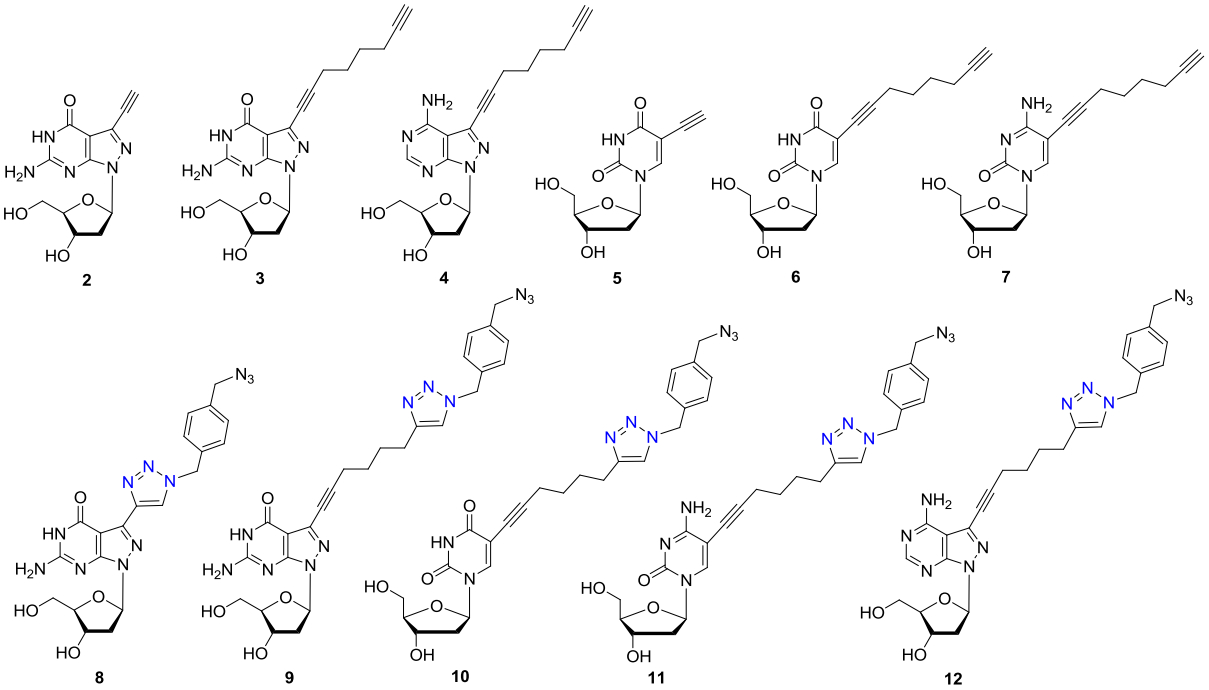

Figure S1. Structures of the alkynylated 2'-deoxyribonucleosides **2-7** and the mono-functionalized azido nucleosides **8-12**.[1-6]

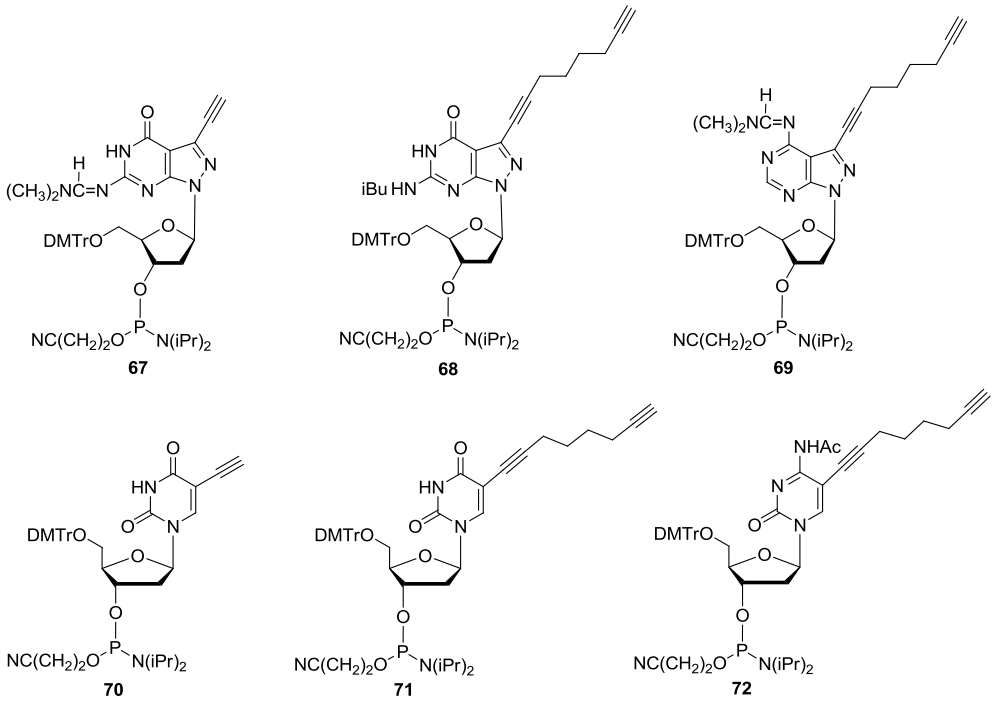

Figure S2. Structures of the phosphoramidite building blocks **67-72** used in this study.[1-6]

Table S1. ^{13}C NMR Chemical Shifts of 5-(Octa-1,7-diynyl)-2'-deoxyuridine Nucleosides.[a]

	C(2)	C(4)	C(5)	C(6)	C≡C	CH_2	Triazole	C(1')	C(2')	C(3')	C(4')	C(5')
6 [5]	149.4	161.7	98.9	142.6	92.9, 84.2, 72.9, 71.3	27.2, 27.1, 18.3, 17.2	-	84.6	[b])	70.2	87.5	60.9
10	149.5	161.8	99.0	147.1	93.1, 73.0	28.1, 27.7, 24.5, 18.6	142.8, 122.1	84.6	[b])	70.2	87.6	61.0

[a] Measured in DMSO-d_6 at 298 K. [b] Superimposed by the DMSO signal.

Table S2. ^{1}H-^{13}C Coupling Constants of 5-(Octa-1,7-diynyl)-2'-deoxyuridine Nucleosides.[a]

^{1}H-^{13}C-coupling constants	*J* [Hz]	
	6 [5]	**10**
^{1}J(C1', H-C1')	168.5	169.9
^{1}J(C3', H-C3')	149.2	149.6
^{1}J(C4', H-C4')	147.6	148.4
^{1}J(C5', H-C5')	141.1	140.8
^{1}J(Triazole-C5, H-C5)	-	182.3

[a] Measured in DMSO-d_6 at 298 K.

Table S3. T_m-values of duplexes containing the alkynylated nucleosides **2-7** as well as azido-functionalized nucleoside derivatives **8-12**.

Duplexes	T_m [a] [°C]	ΔT_m [°C]	% h [b]	$\Delta G°_{310}$ [c] [kcal/mol]	MS[calc.] found	Duplexes	T_m [a] [°C]	ΔT_m [°C]	% h [b]	$\Delta G°_{310}$ [c] [kcal/mol]
5'-d(TAG GTC AAT ACT) (**13**) 3'-d(ATC CAG TTA TGA) (**14**)	51.0 (49.0)	---	18 15	-11.4 -10.8	---					
5'-d(TAG **3**TC AAT ACT) (**18**) 3'-d(ATC CAG TTA TGA) (**14**)	52.0 [3]	+1	18	-11.7	[3746.7] [f] 3748.6 [g]	5'-d(TAG **2**TC AAT ACT) (**16**) 3'-d(ATC CA**2** TTA TGA) (**24**)	57.0	+6	18	-12.8
5'-d(TAG **9**TC AAT ACT) (**31**) 3'-d(ATC CAG TTA TGA) (**14**)	48.5 [3] (46.5)	-2.5 -2.5	20 19	-10.8 -10.3	[3934.8] [f] 3934.8 [g]	5'-d(TAG **2**TC AAT ACT) (**16**) 3'-d(ATC CA**3** TTA TGA) (**25**)	54.5	+3.5	18	-12.2
5'-d(TAG G**6**C AAT ACT) (**22**) 3'-d(ATC CAG TTA TGA) (**14**)	52.0 (49.0)	+1.0 0	16 16	-11.9 -11.0	[3735.5] [h] 3733.0 [i]	5'-d(TAG **3**TC AAT ACT) (**18**) 3'-d(ATC CA**3** TTA TGA) (**25**)	55.5	+4.5	19	-13.0
5'-d(TAG G**10**C AAT ACT) (**32**) 3'-d(ATC CAG TTA TGA) (**14**)	48.5 (46.5)	-2.5 -2.5	15 14	-10.8 -10.3	[3923.7] [h] 3922.2 [i]	5'-d(TAG GT**7** AAT ACT) (**23**) 3'-d(ATC CA**2** TTA TGA) (**24**)	55.5	+4	18	-13.0
5'-d(TAG GT**7** AAT ACT) (**23**) 3'-d(ATC CAG TTA TGA) (**14**)	53.0 (50.5)	+2.0 +1.5	17 17	-12.1 -11.1	[3749.6] [h] 3749.0 [i]	5'-d(TAG **2**TC AAT ACT) (**16**) 3'-d(AT**7** CAG TTA TGA) (**27**)	55.0	+4	19	-12.7
5'-d(TAG GT**11** AAT ACT) (**33**) 3'-d(ATC CAG TTA TGA) (**14**)	49.0 (46.0)	-2.0 -3.0	17 16	-10.8 -10.1	[3934.8] [h] 3928.0 [i]	5'-d(TAG **3**TC AAT ACT) (**18**) 3'-d(AT**7** CAG TTA TGA) (**27**)	53.5	+2.5	19	-12.3
5'-d(TAG GTC **4**AT ACT) (**19**) 3'-d(ATC CAG TTA TGA) (**14**)	51.5 (49.5)	+0.5 +0.5	17 16	-11.6 -11.1	[3749.6] [h] 3751.1 [i]	5'-d(TAG G**6**C AAT ACT) (**22**) 3'-d(ATC CA**2** TTA TGA) (**24**)	54.5	+3.5	18	-12.8
5'-d(TAG GTC**12**AT ACT) (**34**) 3'-d(ATC CAG TTA TGA) (**14**)	47.5 (45.5)	-3.5 -3.5	17 17	-10.4 -9.9	[3937.8] [h] 3939.4 [i]	5'-d(TAG G**6**C AAT ACT) (**22**) 3'-d(ATC CA**3** TTA TGA) (**25**)	52.0	+1	18	-11.8
5'-d(TAG GTC AAT ACT) (**13**) 3'-d(ATC CA**2** TTA TGA) (**24**)	53.5 [3]	+2.5	17	-12.0	[3667.4] [d] 3667.2 [e]	5'-d(TAG G**6**C AAT ACT) (**22**) 3'-d(AT**7** CAG TTA TGA) (**27**)	53.0	+2	17	-12.2
5'-d(TAG GTC AAT ACT) (**13**) 3'-d(ATC CA**8** TTA TGA) (**35**)	48.0 [3] (47.0)	-3.0 -2.0	16 13	-10.5 -10.5	[3855.6] [d] 3855.1 [e]	5'-d(**6**AG GTC AAT ACT) (**21**) 3'-d(AT**7** CAG TTA TGA) (**27**)	53.5	+2.5	18	-12.2
5'-d(TAG GTC AAT ACT) (**13**) 3'-d(ATC CA**3** TTA TGA) (**25**)	51.0 [3]	0	15	-11.4	[3747.6] [d] 3746.9 [e]	5'-d(TAG GT**7** AAT ACT) (**23**) 3'-d(AT**7** CAG TTA TGA) (**27**)	54.0	+3	17	-12.2
5'-d(TAG GTC AAT ACT) (**13**) 3'-d(ATC CA**9** TTA TGA) (**36**)	47.5 [3] (45.5)	-3.5 -3.5	14 17	-10.4 -9.9	[3934.8] [f] 3934.7 [g]	5'-d(TAG **9**TC AAT ACT) (**31**) 3'-d(ATC CA**3** TTA TGA) (**25**)	53.5 (52.0)	+2.5 +3.0	18 17	-11.8 -11.5

5’-d(**6**AG GTC AAT ACT) (**21**) 3’-d(ATC CAG TTA TGA) (**14**)	52.5 50.0	+1.5 +1	17 18	-12.1 -11.1	[3735.5][h] 3731.0[i]	5’-d(TAG G**10**C AAT ACT) (**32**) 3’-d(ATC CA**3** TTA TGA) (**25**)	50.0 (48.5)	-1.0 -0.5	15 14	-11.2 -10.9
5’-d(**10**AG GTC AAT ACT) (**37**) 3’-d(ATC CAG TTA TGA) (**14**)	53.5 (52.5)	+2.5 +3.5	17 14	-13.2 -12.2	[3923.7][h] 3926.7[i]	5’-d(TAG GT**11** AAT ACT) (**33**) 3’-d(ATC CA**3** TTA TGA) (**25**)	50.0 (48.0)	-1.0 -1.0	17 17	-11.1 -10.5
5’-d(TAG GTC AAT ACT) (**13**) 3’-d(A**6**C CAG TTA TGA) (**26**)	51.5 49.0	+0.5 0	18 16	-11.4 -10.8	[3735.5][h] 3733.7[i]	5’-d(TAG GTC **12**AT ACT) (**34**) 3’-d(ATC CA**3** TTA TGA) (**25**)	49.5 (47.5)	-1.5 -1.5	15 14	-11.0 -10.5
5’-d(TAG GTC AAT ACT) (**13**) 3’-d(A**10**C CAG TTA TGA) (**38**)	52.5 (50.5)	+1.5 +1.5	14 17	-12.2 -12.0	[3923.7][h] 3921.0[i]	5’-d(TAG **2**TC AAT ACT) (**16**) 3’-d(ATC CA**8** TTA TGA) (**35**)	54.5	+3.5	19	-12.3
5’-d(TA**2** GTC AAT ACT) (**15**) 3’-d(ATC CA**2** TTA TGA) (**24**)	55.0	+4	19	-12.8	[3666.7][f] 3668.6[g] (ODN-**15**)	5’-d(TAG **2**TC AAT ACT) (**16**) 3’-d(ATC CA**9** TTA TGA) (**36**)	52.0	+1.0	17	-11.8
5’-d(**5**AG GTC AAT ACT) (**20**) 3’-d(A**6**C CAG TTA TGA) (**26**)	50.0 (49.0)	-1.0 0	18 18	-11.0 -10.9	[3655.4][h] 3655.2[i] (ODN-**20**)	5’-d(**10**AG GTC AAT ACT) (**37**) 3’-d(ATC CA**2** TTA TGA) (**24**)	55.5	+4.5	19	-12.8
5’-d(TA**2** GTC AAT ACT) (**15**) 3’-d(AT**7** CAG TTA TGA) (**27**)	54.5	+3.5	18	-12.4	[3749.6][h] 3748.8[i] (ODN-**27**)	5’-d(**5**AG GTC AAT ACT) (**20**) 3’-d(A**10**C CAG TTA TGA) (**38**)	49.5	-1.5	18	-11.2
5’-d(TAG GT**7** AAT ACT) (**23**) 3’-d(ATC **7**AG TTA TGA) (**28**)	52.5	+1.5	18	-11.8	[3749.6][h] 3749.6[i] (ODN-**28**)					
5’-d(TAG GTC **2**AT ACT) (**17**) 3’-d(ATC CA**2** TTA TGA) (**24**)	47.0	-4	17	-10.4	[3682.6][f] 3682.6[g] (ODN-**17**)					
5’-d(TAG**2**TCAATACT) (**16**) 3’-d(T_6ATCCA**3**TTATGAT$_6$) (**29**)	55.0	+4	15	-12.6	[7399.9][h] 7398.9[i] (ODN-**29**)					
5’-d(TAG**2**TCAATACT) (**16**) 3’-d(A_6ATCCA**3**TTATGAT$_6$) (**30**)	55.5	+4.5	14	-12.4	[7452.0][d] 7452.4[e] (ODN-**30**)					

[a] Measured at 260 nm in a 1 M NaCl solution containing 100 mM $MgCl_2$ and 60 mM Na-cacodylate (pH 7.0) with 5 µM + 5 µM single-strand concentration. Data in parentheses were measured at a 2 µM + 2 µM single-strand concentration. [b] % h refers to the percentage of hypochromicity. [c] $\Delta G°_{310}$ values are given with 15% error. [d] Calculated on the basis of molecular weight as $[M-1]^-$. [e] Determined by MALDI-TOF mass spectrometry as $[M-1]^-$ in the linear negative mode. [f] Calculated on the basis of exact mass. [g] Determined by LC-ESI-TOF mass spectrometry. [h] Calculated on the basis of molecular weight as $[M+1]^+$. [i] Determined by MALDI-TOF mass spectrometry as $[M+1]^+$ in the linear positive mode.

Table S4. Structure and and mass spectrometrical data of the cross-linked duplexes **ICL-39** to **ICL-66**.

Duplexes DNA (ICL)	MS (calc.) found	Duplexes DNA (ICL)	MS (calc.) found
5'-d(TAG **3**TC AAT ACT) 3'-d(ATC CA**3** TTA TGA) **(39)**	[7681.5] [c] 7685.5 [d]	5'-d(TAG GT**7** AAT ACT) 3'-d(ATC CA**2** TTA TGA) **(51)**	[7604.2] [e] 7604.2 [f]
5'-d(TAG G**6**C AAT ACT) 3'-d(ATC CA**3** TTA TGA) **(40)**	[7667.5] [c] 7669.4 [d]	5'-d(TA**2** GTC AAT ACT) 3'-d(AT**7** CAG TTA TGA) **(52)**	[7601.5] [c] 7605.4 [d]
5'-d(TAG GT**7** AAT ACT) 3'-d(ATC CA**3** TTA TGA) **(41)**	[7685.3] [a] 7688.3 [b]	5'-d(TAG **2**TC AAT ACT) 3'-d(AT**7** CAG TTA TGA) **(53)**	[7601.5] [c] 7603.5 [d]
5'-d(TAG GTC **4**AT ACT) 3'-d(ATC CA**3** TTA TGA) **(42)**	[7686.3] [a] 7689.2 [b]	5'-d(TAG **3**TC AAT ACT) 3'-d(AT**7** CAG TTA TGA) **(54)**	[7680.5] [c] 7685.5 [d]
5'-d(TAG **2**TC AAT ACT) 3'-d(ATC CA**2** TTA TGA) **(43)**	[7521.4] [c] 7524.5 [d]	5'-d(TAG G**6**C AAT ACT) 3'-d(ATC CA**2** TTA TGA) **(55)**	[7587.5] [c] 7589.5 [d]
5'-d(TAG **2**TC AAT ACT) 3'-d(ATC CA**3** TTA TGA) **(44)**	[7601.5] [c] 7604.5 [d]	5'-d(TAG G**6**C AAT ACT) 3'-d(AT**7** CAG TTA TGA) **(56)**	[7667.5] [c] 7673.5 [d]
5'-d(**6**AG GTC AAT ACT) 3'-d(ATC CA**2** TTA TGA) **(45)**	[7594.2] [a] 7599.7 [b]	5'-d(**6**AG GTC AAT ACT) 3'-d(AT**7** CAG TTA TGA) **(57)**	[7667.5] [c] 7670.3 [d]
5'-d(**5**AG GTC AAT ACT) 3'-d(A**6**C CAG TTA TGA) **(46)**	[7578.1] [a] 7575.0 [b]	5'-d(TAG G T**7** AAT ACT) 3'-d(AT**7** CAG TTA TGA) **(58)**	[7681.5] [c] 7682.3 [d]
5'-d(TA**2**G TC AAT ACT) 3'-d(ATC CA**2**TTA TGA) **(47)**	[7521.4] [c] 7523.3 [d]	5'-d(TAG GT**7** AAT ACT) 3'-d(ATC **7**AG TTA TGA) **(59)**	[7681.5] [c] 7682.5 [d]
5'-d(TAG GTC **2**AT ACT) 3'-d(ATC CA**2** TTA TGA) **(48)**	[7537.4] [c] 7539.3 [d]	5'-d(AGT ATT **2**AC CTA) 5'-d(A**2**T ATT GAC CTA) **(66)** [3]	[7521.4] [c] 7524.2 [d]
5'-d(TAG **2**TC AAT ACT) 3'-d(TTTTTT ATC CA**3** TTA TGA TTTTTT) **(49)**			[11250.0] [c] 11250.9 [d]
5'-d(TAG **2**TC AAT ACT) 3'-d(AAAAAA ATC CA**3** TTA TGA TTTTTT) **(50)**			[11308.6] [c] 11309.0 [d]
5'-d(TAG **2**TC AAT ACT) 5'-d(TAG **2**TC AAT ACT) **(60)** [3]	[7521.4] [c] 7521.3 [d]	5'-d(AGT ATT **3**AC CTA) 5'-d(AGT ATT **3**AC CTA) **(63)** [3]	[7681.5] [c] 7685.3 [d]
5'-d(AGT ATT **2**AC CTA) 5'-d(AGT ATT **2**AC CTA) **(61)** [3]	[7521.4] [c] 7524.3 [d]	5'-d(TAG GT**7** AAT ACT) 5'-d(TAG GT**7** AAT ACT) **(64)**	[7686.3] [a] 7688.0 [b]
5'-d(TAG G**6**C AAT ACT) 5'-d(TAG G**6**C AAT ACT) **(62)**	[7658.3] [a] 7658.0 [b]	5'-d(AGT ATT GA**7** CTA) 5'-d(AGT ATT GA**7** CTA) **(65)**	[7686.3] [a] 7688.0 [b]

[a] Calculated on the basis of molecular weight as $[M+1]^+$. [b] Determined by MALDI-TOF mass spectrometry as $[M+1]^+$ in the linear positive mode. [c] Calculated on the basis of exact mass. [d] Determined by LC-ESI-TOF mass spectrometry. [e] Calculated on the basis of molecular weight as $[M-1]^-$. [f] Determined by MALDI-TOF mass spectrometry as $[M-1]^-$ in the linear negative mode.

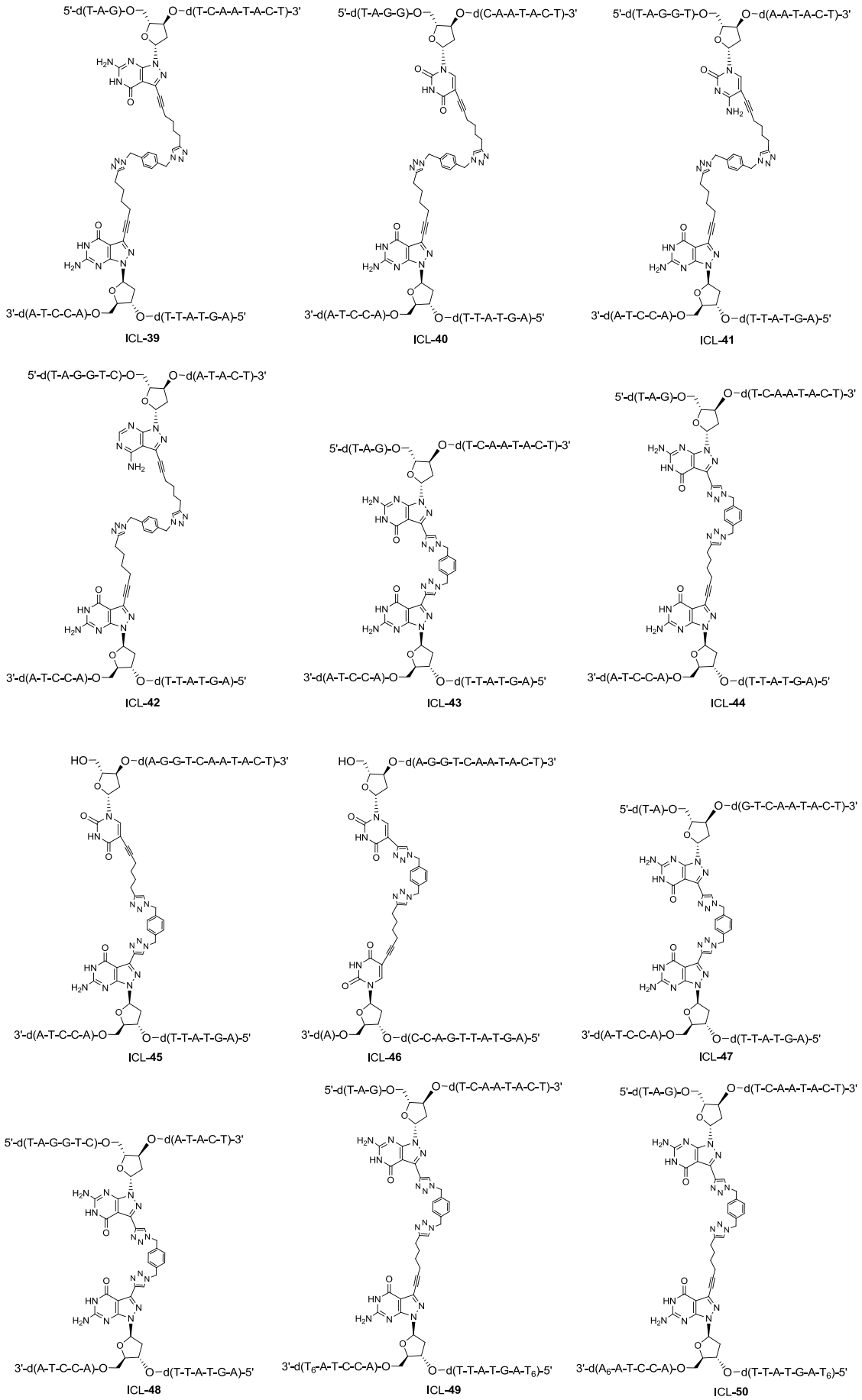

Figure S3. Structures of the interstrand cross-linked duplexes ICL-**39** to ICL-**50**.

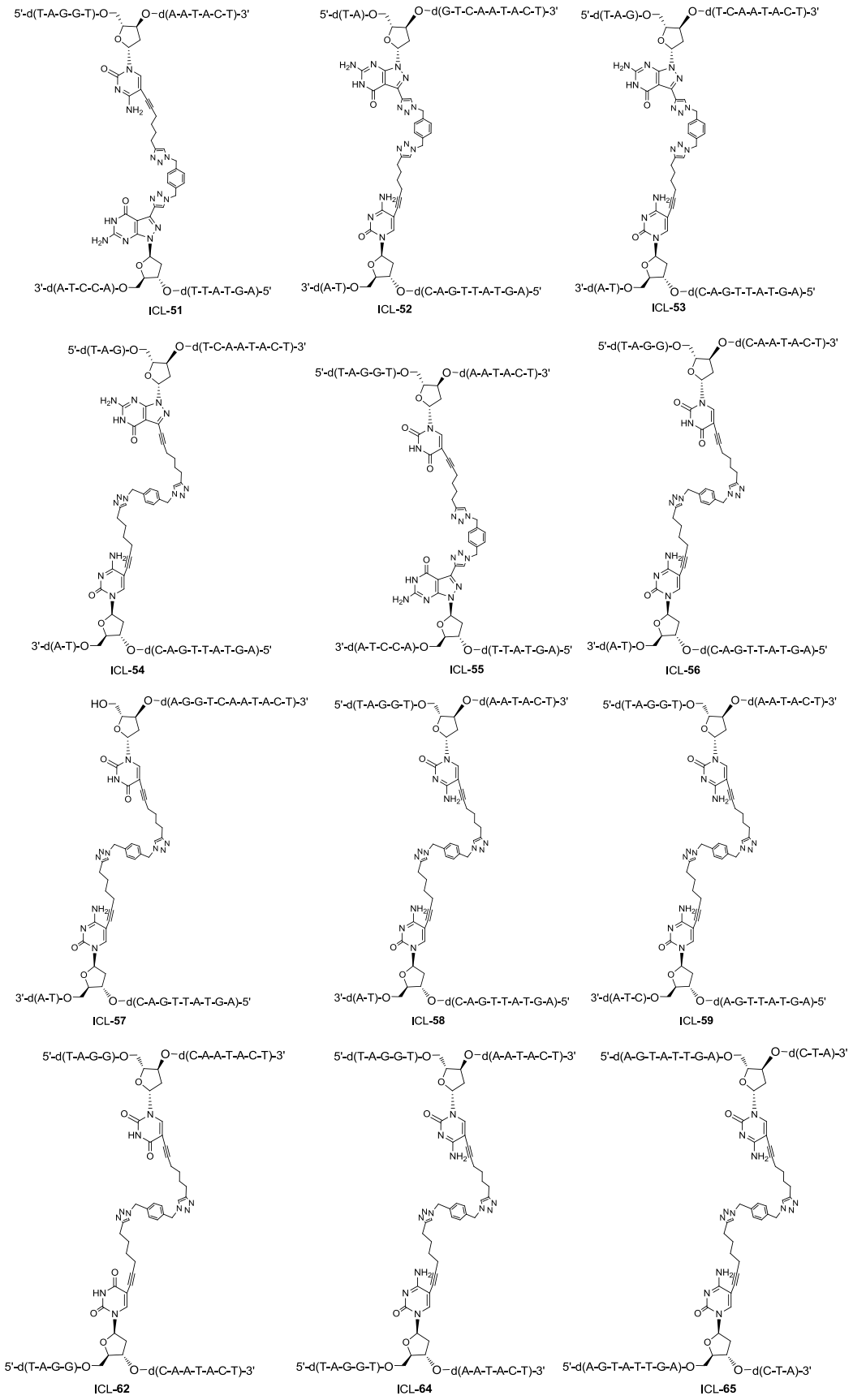

Figure S4. Structures of the interstrand cross-linked duplexes ICL-**51** to ICL-**59**, ICL-**62**, ICL-**64** and ICL-**65**.

HPLC Profiles of Modified Oligonucleotides and Cross-linked Oligonucleotides:

Figure S5-S9: HPLC (RP-18) profiles of modified single-stranded oligonucleotides (ODNs) or interstrand cross-linked oligonucleotides (ICL) measured at 260 nm. The following solvent system was used: MeCN (A) and 0.1 M (Et_3NH)OAc (pH 7.0) (B). Gradient *III*: 0-15 min 0-20% A, 15-18 min 20-40% A in B, 18-20 min 40-0% A in B, 20-25 min 40-0% A in B with a flow rate of 0.7 mL min^{-1}.

Figure S10-S12: Ion-exchange HPLC elution profiles of the modified single-stranded oligonucleotides (ODN) or interstrand cross-linked oligonucleotides (ICL) on a 4 × 250 mm DNA PA-100 column using the following buffer system: Gradient *IV*: (C) 25 mM Tris-HCl, 10% MeCN, pH 7.0; (D) 25 mM Tris-HCl, 1.0 M NaCl, and 10% MeCN, pH 7.0. Elution gradient *IV*: 0-30 min 20-80% D in C with a flow rate of 0.75 mL min^{-1}.

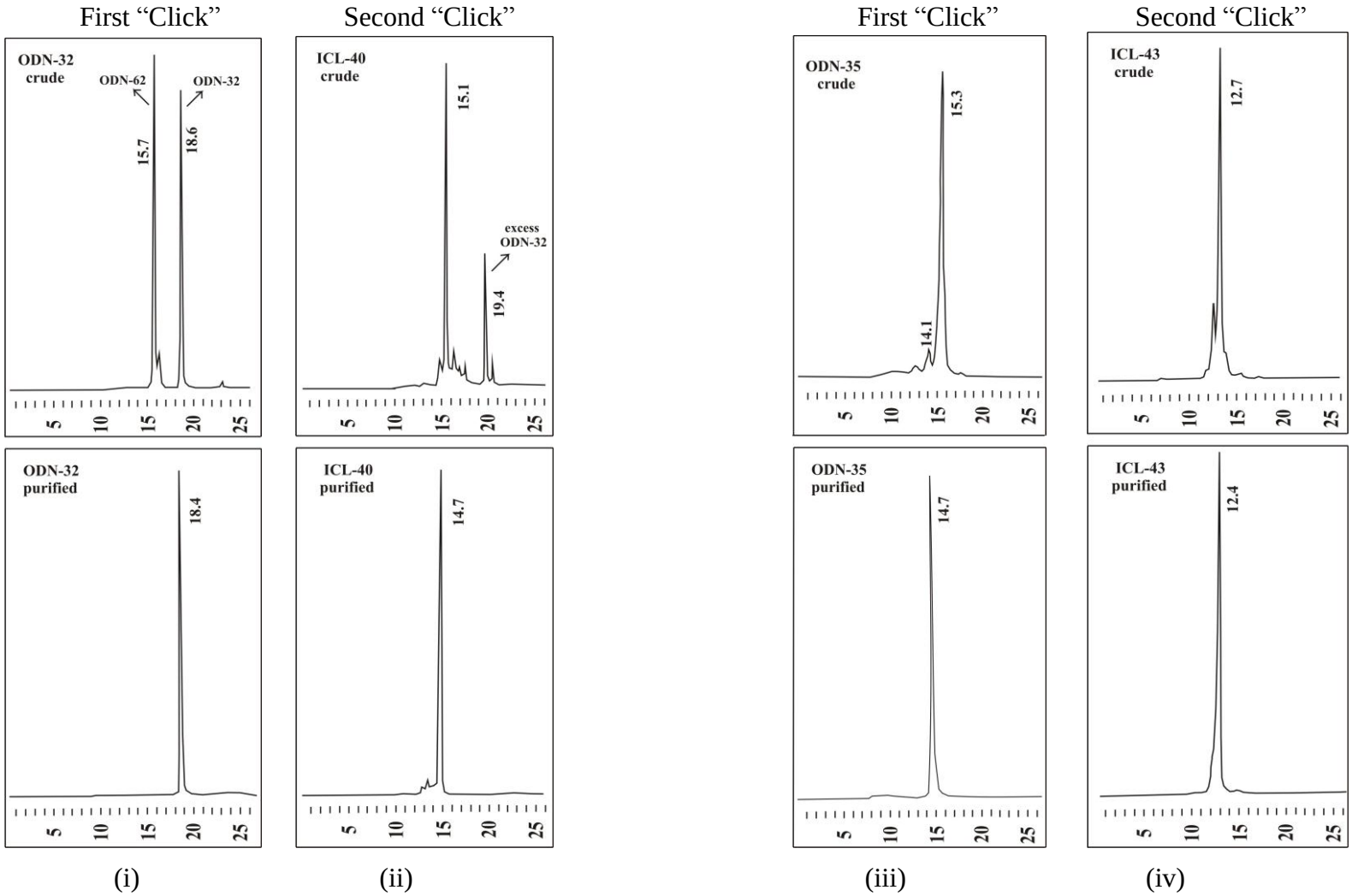

Figure S5. Reversed-phase HPLC profiles of the crude azidomethylbenzyl-labeled ODN-**32** (i) and ODN-**35** (iii) obtained from the “first click” of the “stepwise click” reaction before (first row) and after purification (second row). HPLC profiles of the “second click” reaction with ODN-**32** (i) or ODN-**35** (iii) as starting materials, and ODN-**25** or ODN-**16** as the second component, yielding the interstrand cross-linked ICL-**40** (ii) or ICL-**43** (iv) before (first row) and after purification (second row).

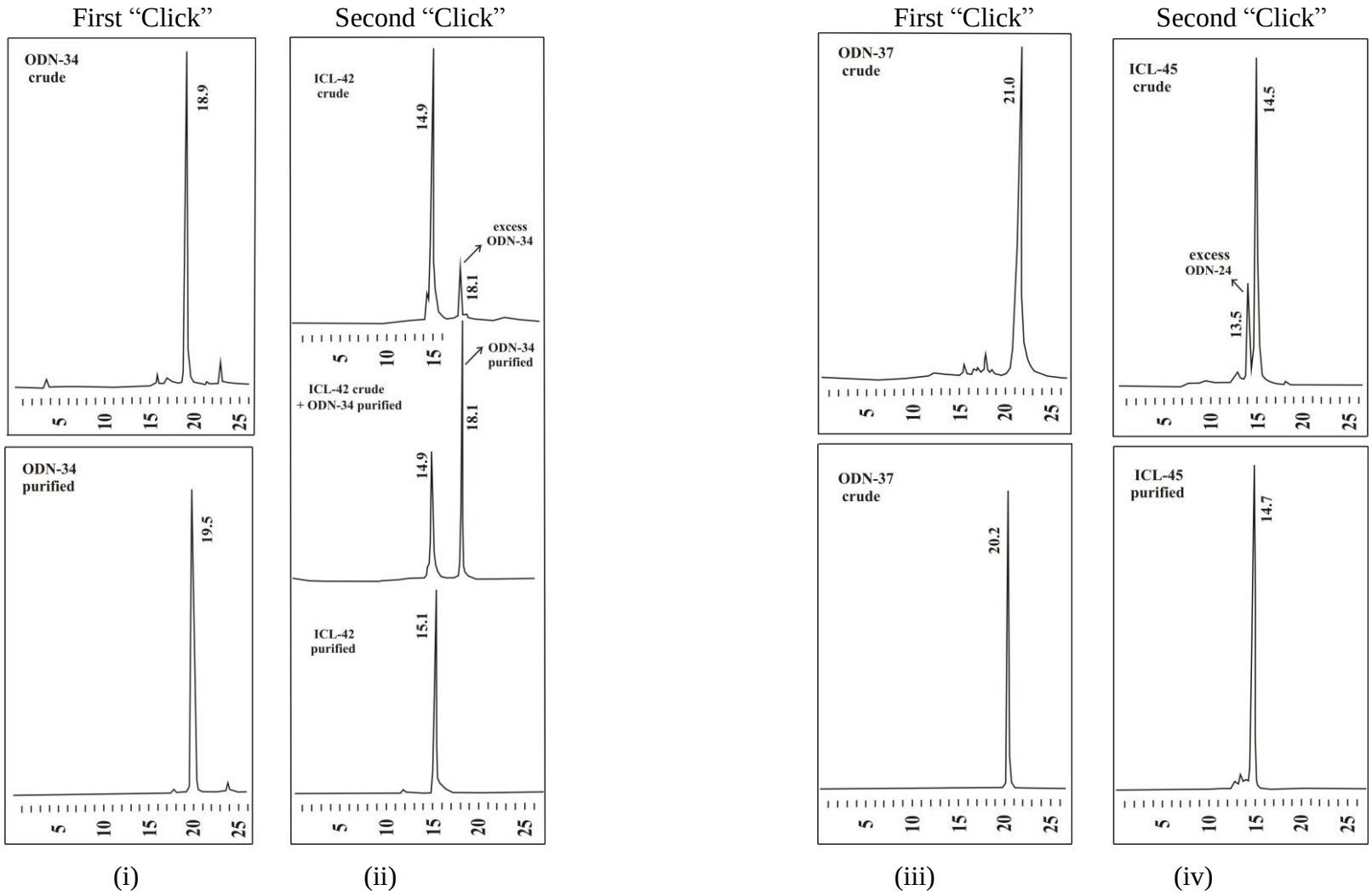

Figure S6. Reversed-phase HPLC profiles of the crude azidomethylbenzyl-labeled ODN-**34** (i) and ODN-**37** (iii) obtained from the "first click" of the "stepwise click" reaction before (first row) and after purification (second row). HPLC profiles of the "second click" reaction with ODN-**34** (i) or ODN-**37** (iii) as starting materials, and ODN-**25** or ODN-**24** as the second component, yielding the interstrand cross-linked ICL-**42** (ii) or ICL-**45** (iv) before (first row) and after purification (second row).

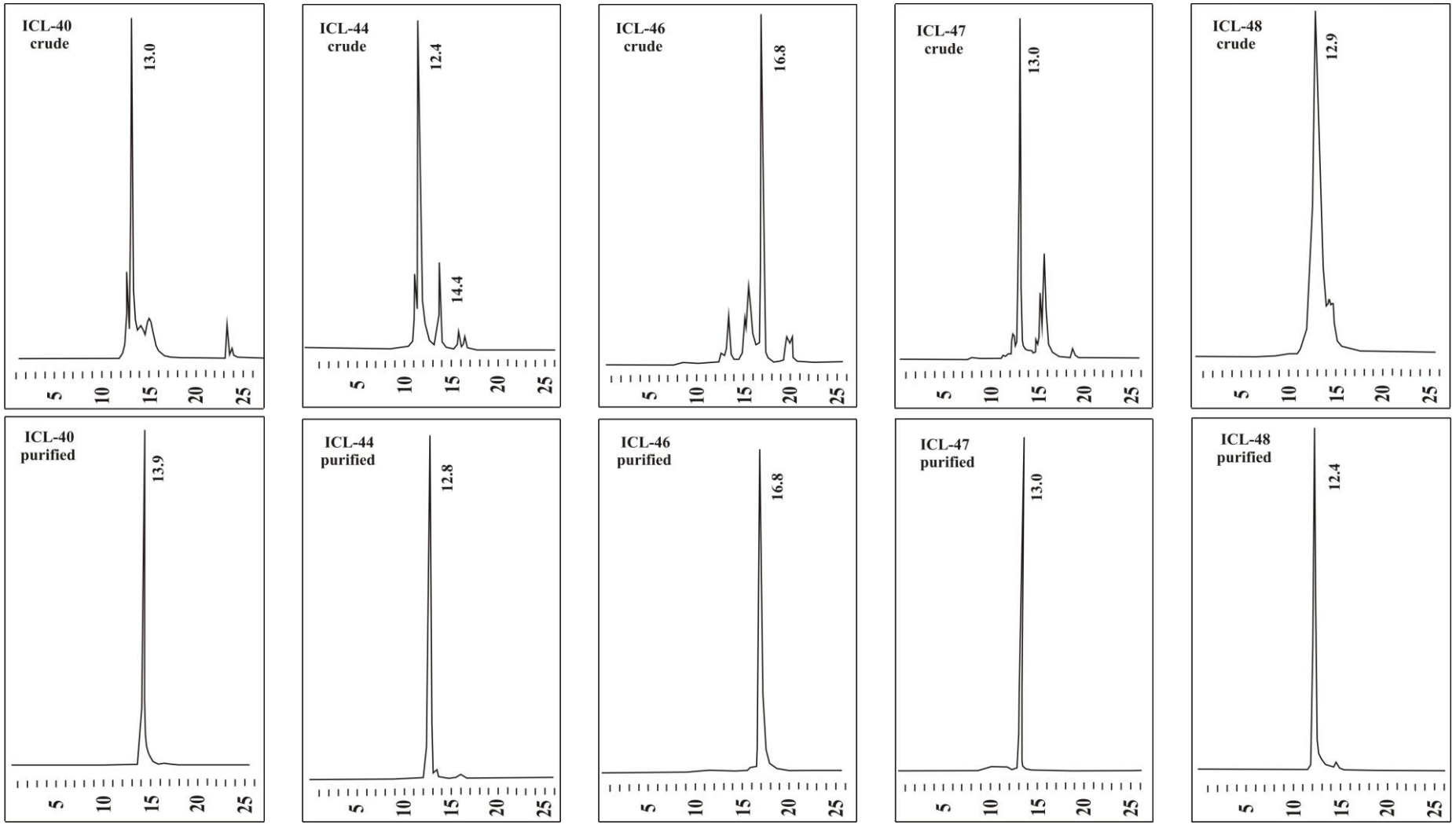

(a) ICL-**40** (b) ICL-**44** (c) ICL-**46** (d) ICL-**47** (e) ICL-**48**

Figure S7. Reversed-phase HPLC profiles of the interstrand cross-linked oligonucleotides ICL-**40**, ICL-**44** and ICL-**46** to ICL-**48** before (first row) and after (second row) purification.

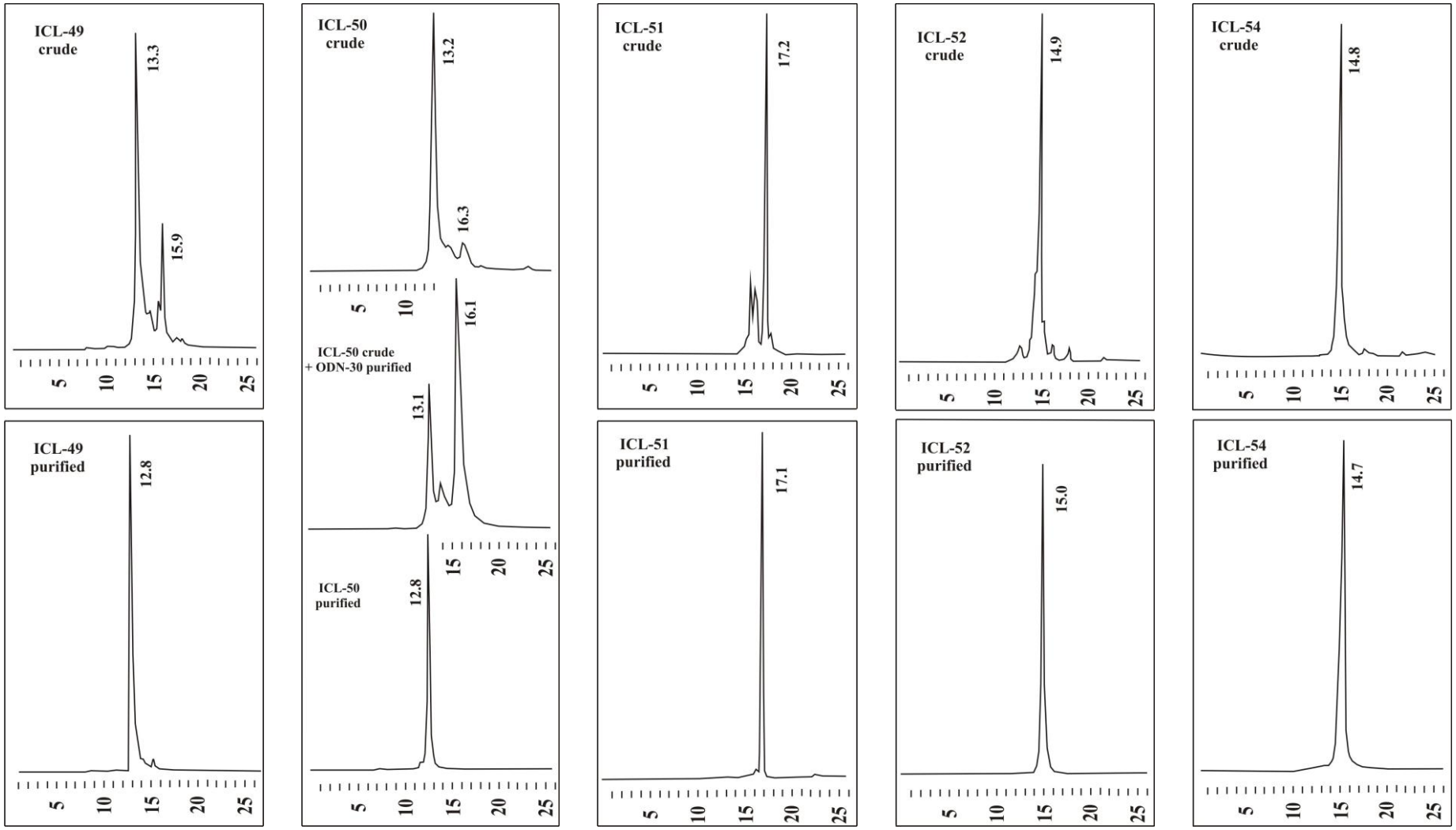

(a) ICL-**49** (b) ICL-**50** (c) ICL-**51** (d) ICL-**52** (e) ICL-**54**

Figure S8. Reversed-phase HPLC profiles of the interstrand cross-linked oligonucleotides ICL-**49** to ICL-**52** and ICL-**54** before (first row) and after (second row) purification.

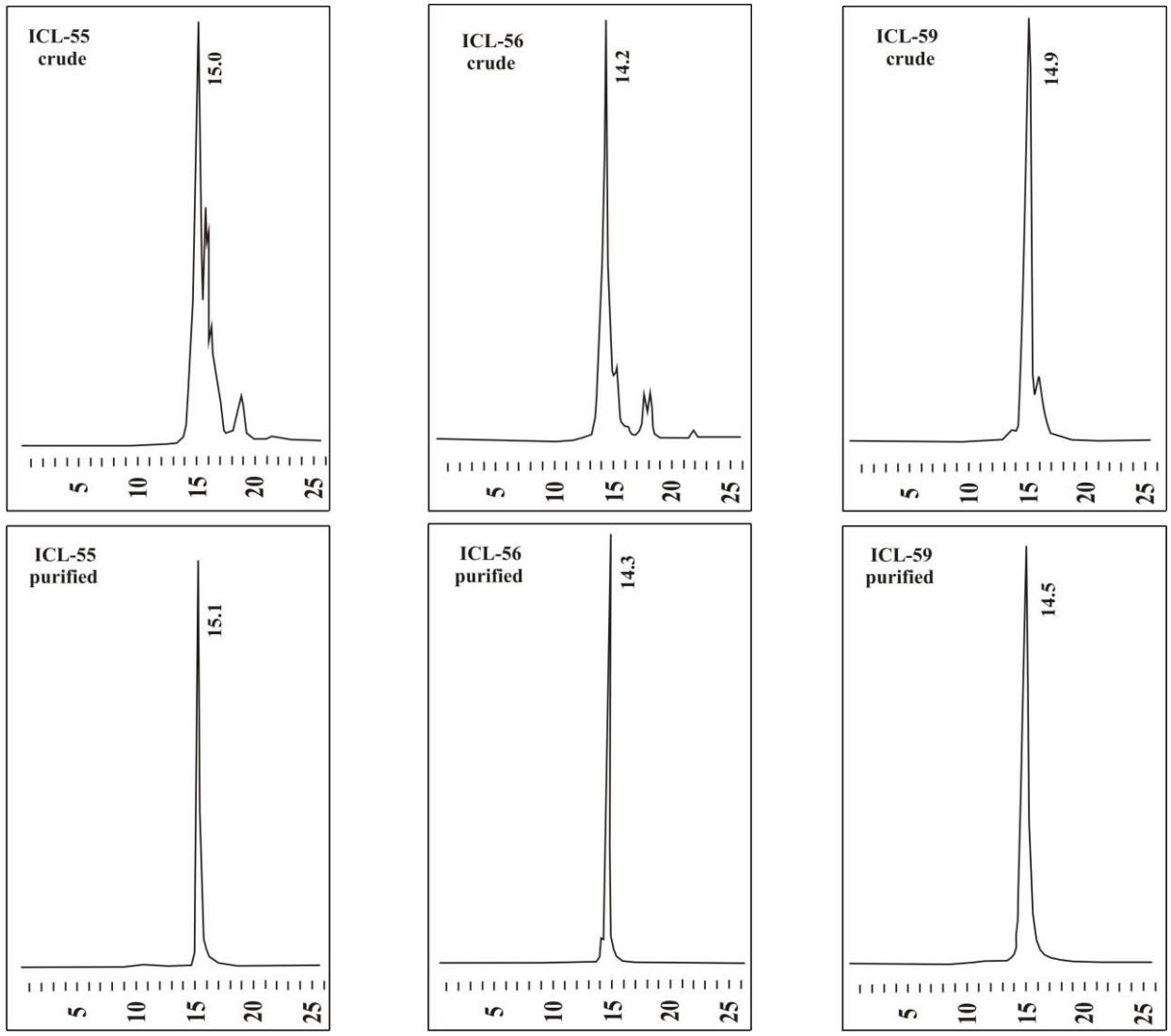

(a) ICL-**55** (b) ICL-**56** (c) ICL-**59**

Figure S9. Reversed-Phase HPLC profiles of the interstrand cross-linked oligonucleotides ICL-**55**, ICL-**56** and ICL-**59**.

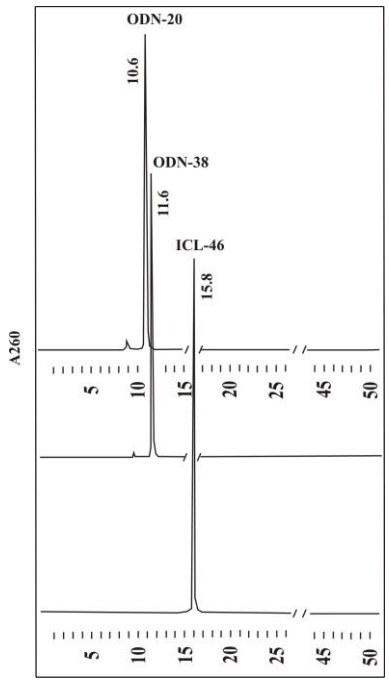

Figure S10. Ion-exchange HPLC elution profiles of ODN-**20** (upper part), azidomethybenzyl-labeled ODN-**38** (middle part) and the interstrand cross-link ICL-**46** (lower part) on a 4 × 250 mm DNA PA-100 column using the following buffer system: Gradient *IV*.

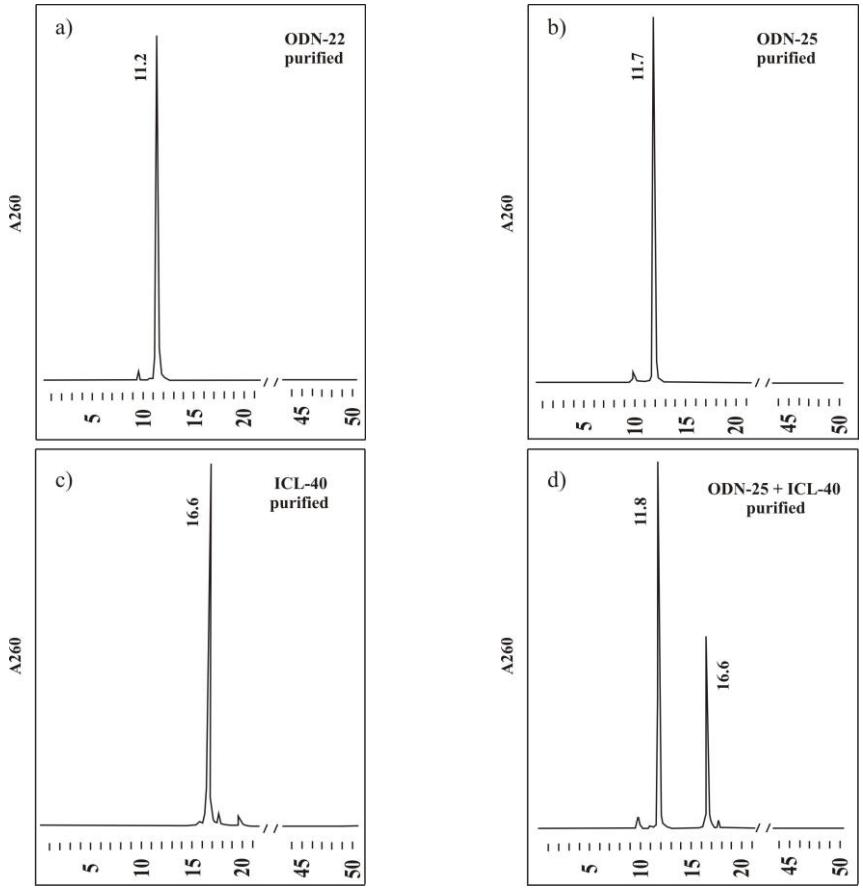

Figure S11. Ion-exchange HPLC elution profiles of (a) ODN-**22**; (b) ODN-**25**; (c) ICL-**40**; (d) artificial mixture of ICL-**40** and ODN-**25** on a 4 × 250 mm DNA PA-100 column using the following buffer system: Gradient *IV*.

.

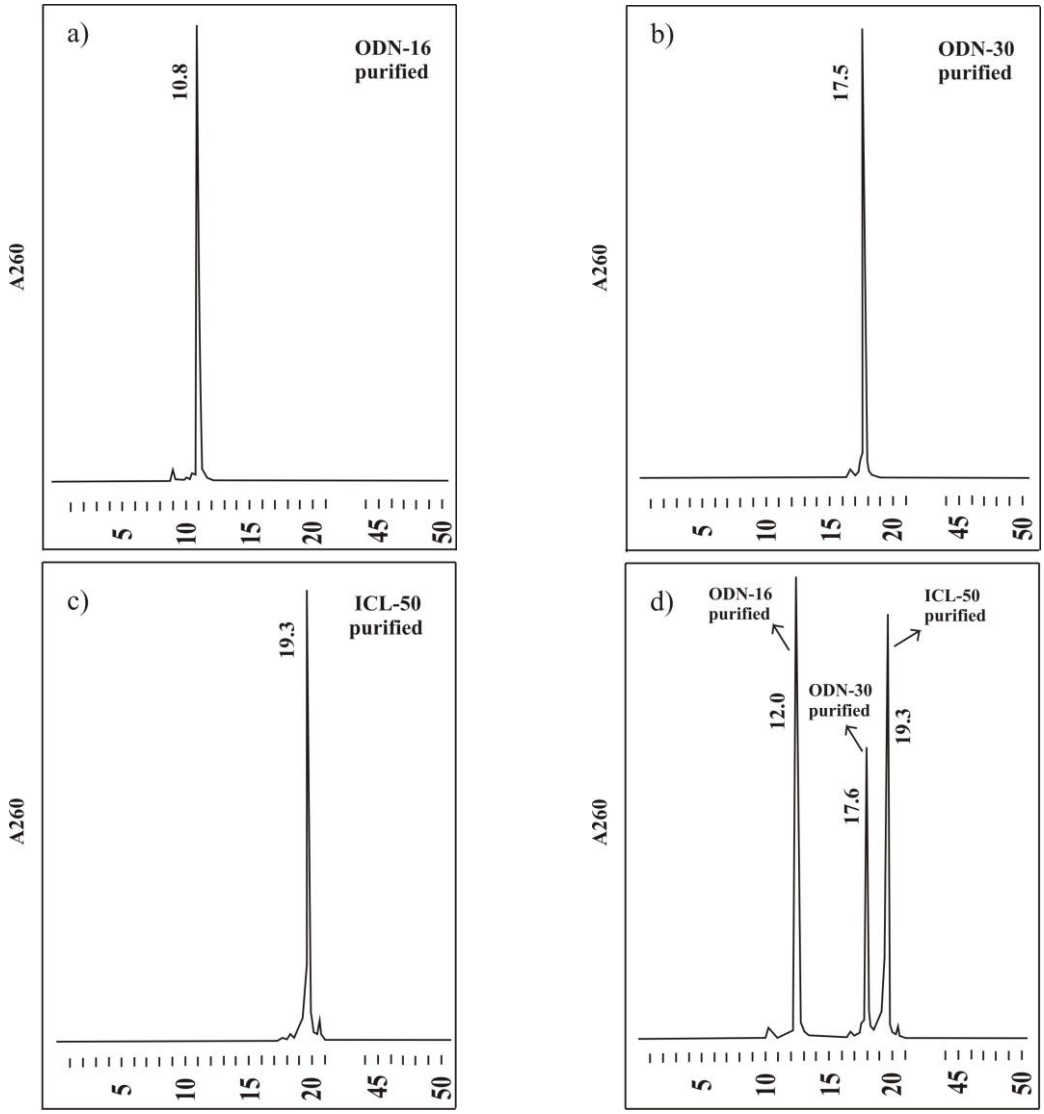

Figure S12. Ion-exchange HPLC elution profiles of (a) ODN-**16**; (b) ODN-**30**; (c) ICL-**50**; (d) artificial mixture of ICL-**50**, ODN-**16** and ODN-**30** on a 4 × 250 mm DNA PA-100 column using the following buffer system: Gradient *IV*.

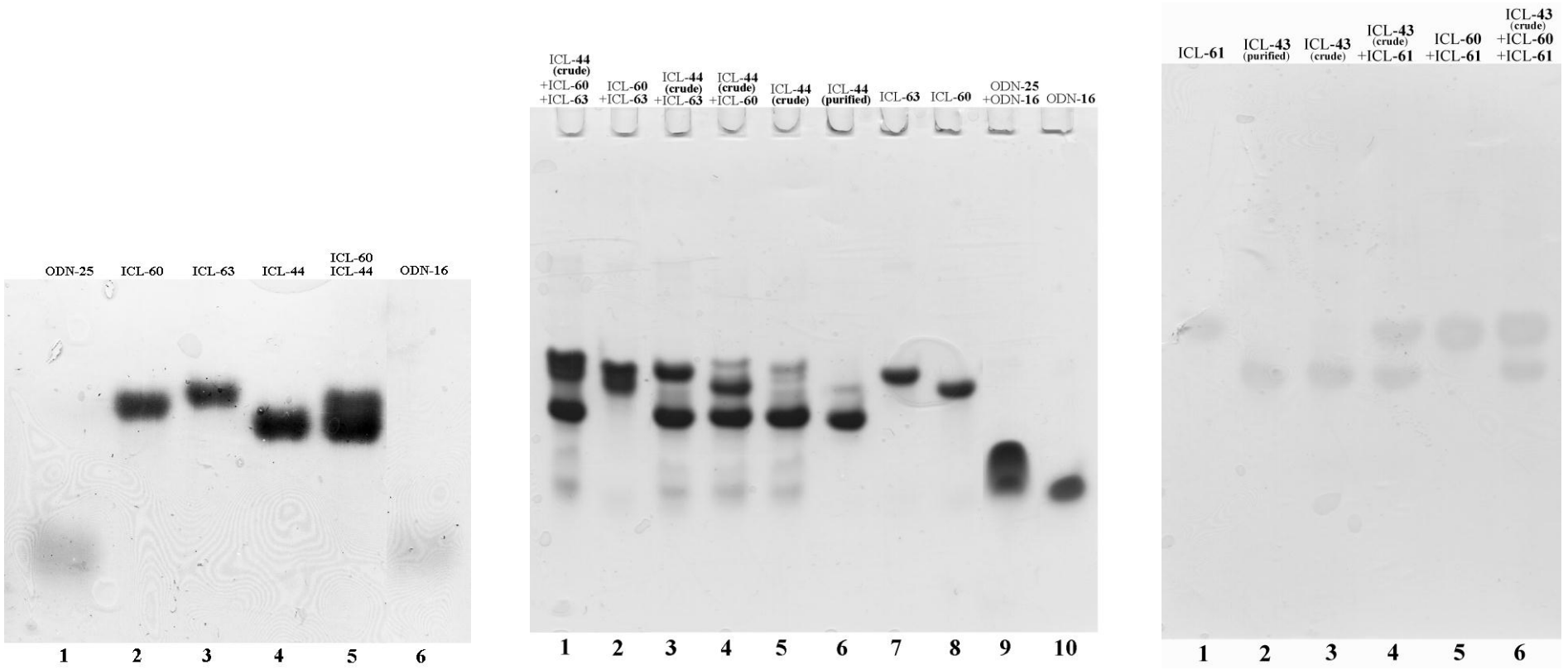

(a) (b) (c)

Figure S13. Denaturing PAGE analysis of oligonucleotides on a 17% polyacrylamide/7 M urea gel (10 x 10 cm). (a) Lane 1: 12-mer ODN-**25**; lane 2: 24-mer homodimer ICL-**60** [3]; lane 3: 24-mer homodimer ICL-**63** [3]; lane 4: 24-mer heterodimer ICL-**44**; lane 5: artificial mixture of ICL-**60** + ICL-**44**; lane 6: 12-mer ODN-**16**. (b) Lane 1: artificial mixture of ICL-**60** + ICL-**63** + ICL-**44** (crude); lane 2: mixture of ICL-**60** + ICL-**63**; lane 3: mixture of ICL-**63** + ICL-**44** (crude); lane 4: mixture of ICL-**60** + ICL-**44** (crude); lane 5: 24-mer heterodimer ICL-**44** (crude); lane 6: 24-mer heterodimer ICL-**44** (purified); lane 7: 24-mer homodimer ICL-**63**; lane 8: 24-mer homodimer ICL-**60**; lane 9: artificial mixture of ODN-**16** + ODN-**25**; lane 10: 12-mer ODN-**16**. (c) Lane 1: 24-mer homodimer ICL-**61**; lane 2: 24-mer heterodimer ICL-**43** (purified); lane 3: 24-mer heterodimer ICL-**43** (crude); lane 4: mixture of ICL-**61** + ICL-**43** (crude); lane 5: mixture of ICL-**60** + ICL-**61**; lane 6: mixture of ICL-**60** + ICL-**61** + ICL-**43** (crude).

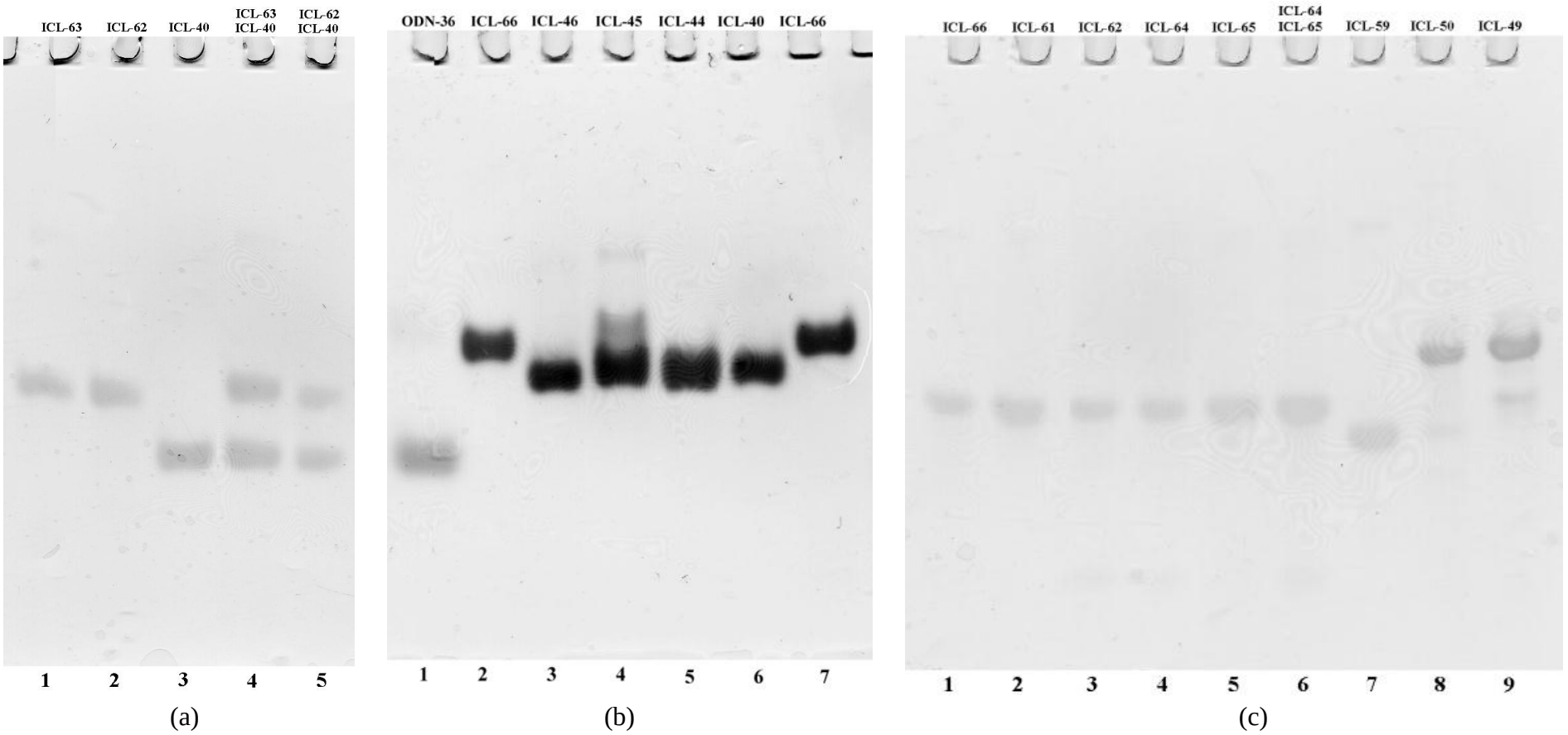

Figure S14. Denaturing PAGE analysis of oligonucleotides on a 17% polyacrylamide/7 M urea gel. (a) Lane 1: 24-mer homodimer ICL-**63**; lane 2: 24-mer homodimer ICL-**62**; lane 3: 24-mer heterodimer ICL-**40**; lane 4: artificial mixture of ICL-**63** + ICL-**40**; lane 5: mixtures of ICL-**62** + ICL-**40**. (b) Lane 1: 12-mer ODN-**36**; lane 2: 24-mer homodimer ICL-**66**; lane 3: 24-mer heterodimer ICL-**46**; lane 4: 24-mer heterodimer ICL-**45**; lane 5: 24-mer heterodimer ICL-**44**; lane 6: 24-mer heterodimer ICL-**40**; lane 7: 24-mer homodimer ICL-**66**. (c) Lane 1: 24-mer homodimer ICL-**66**; lane 2: 24-mer homodimer ICL-**61**; lane 3: 24-mer homodimer ICL-**62**; lane 4: 24-mer homodimer ICL-**64**; lane 5: 24-mer homodimer ICL-**65**; lane 6: mixture of ICL-**64** + ICL-**65**; lane 7: 24-mer heterodimer ICL-**59**; lane 8: 36-mer heterodimer ICL-**50**; lane 9: 36-mer heterodimer ICL-**49**.

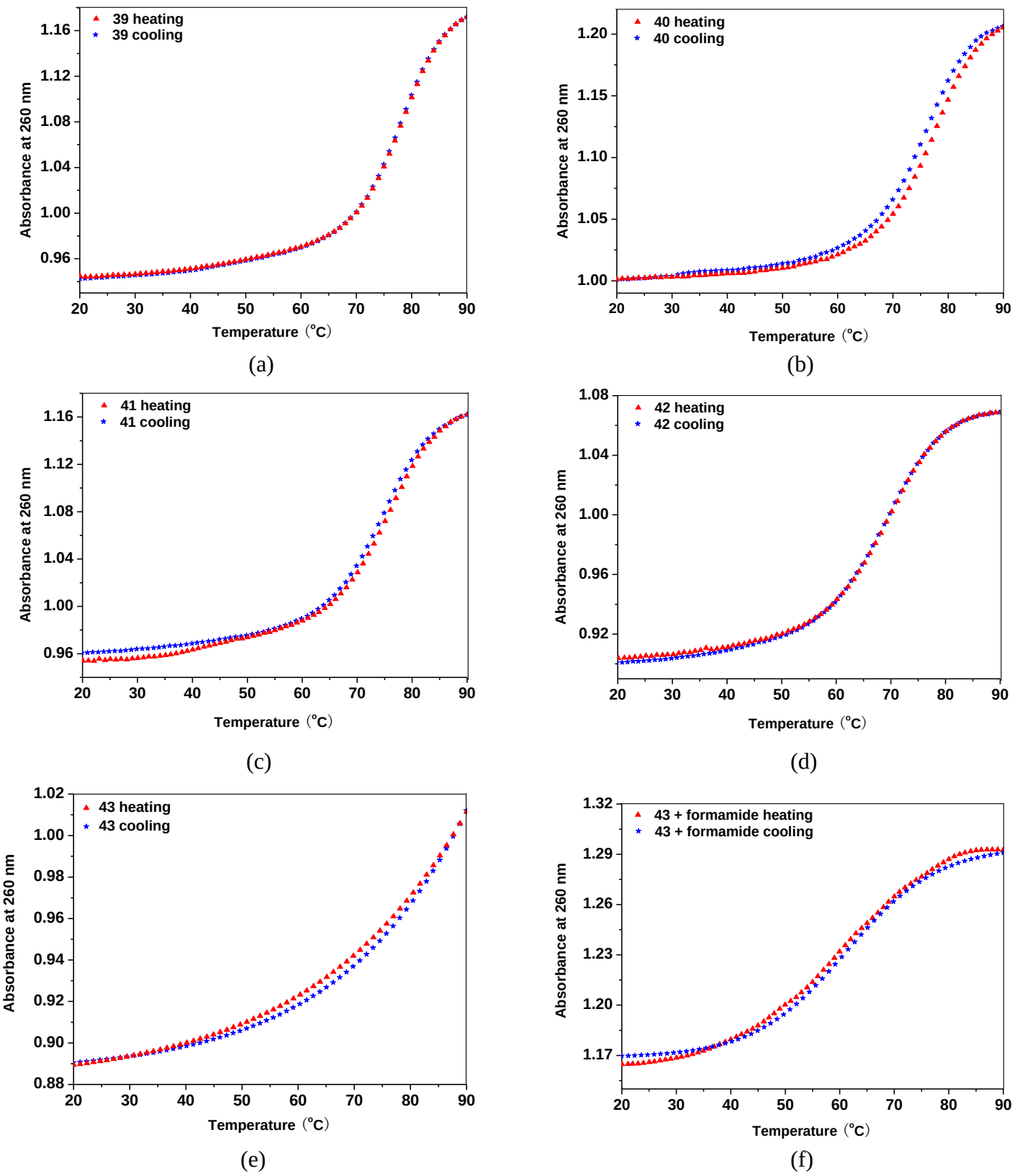

Figure S15. Original melting curves obtained from heating (red triangles) and cooling (blue stars) experiments measured at 260 nm in a 1 M NaCl solution containing 100 mM $MgCl_2$ and 60 mM Na-cacodylate (pH 7.0) with 5 μM of interstrand cross-linked duplex concentration. (a) ICL-**39**; (b) ICL-**40**; (c) ICL-**41**; (d) ICL-**42**; (e) ICL-**43** and (f) ICL-**43** measured in a 1:1 (v/v) mixture of buffer (see above) and formamide.

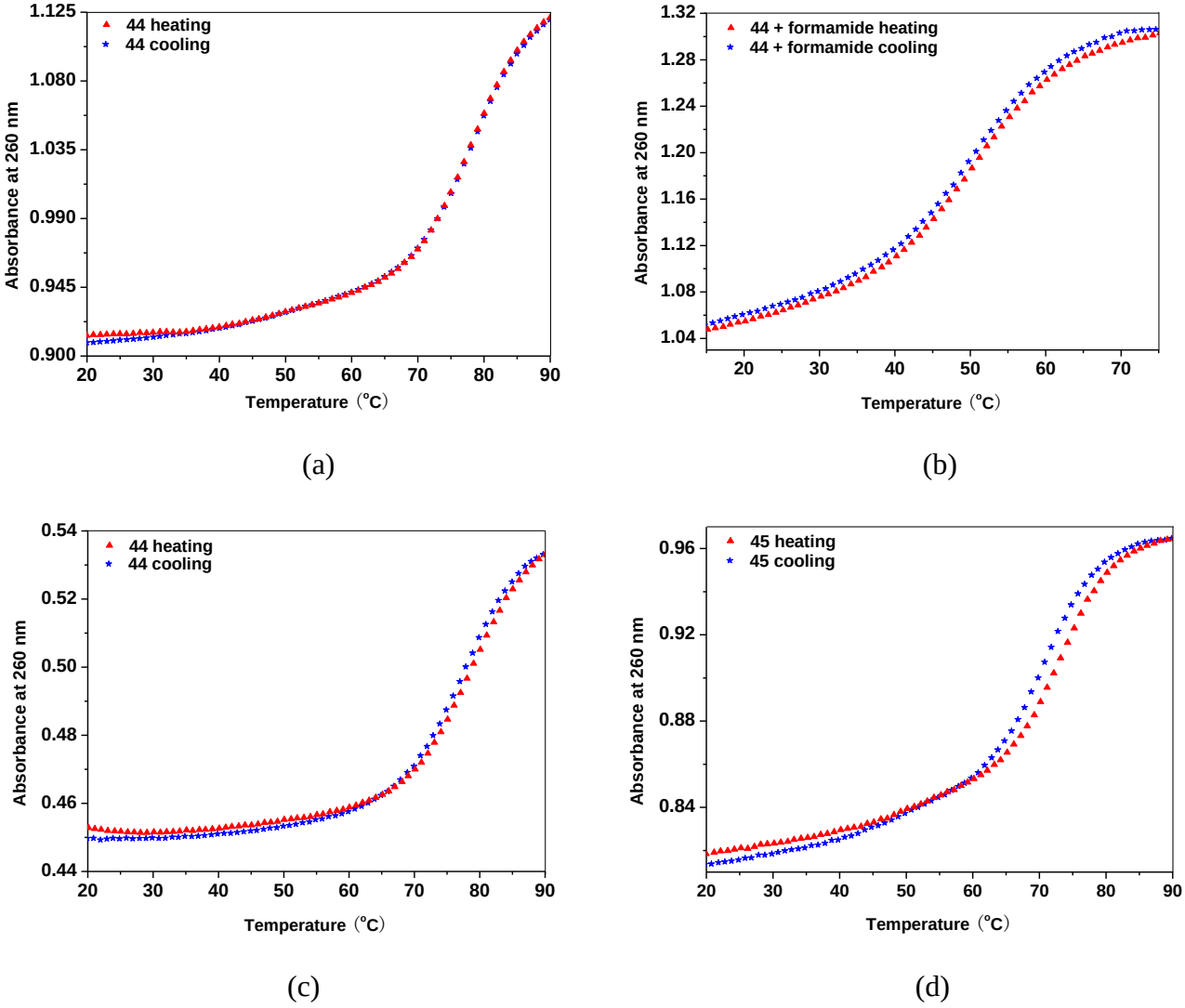

Figure S16. Original melting curves obtained from heating (red triangles) and cooling (blue stars) experiments measured at 260 nm in a 1 M NaCl solution containing 100 mM $MgCl_2$ and 60 mM Na-cacodylate (pH 7.0) with 5 μM of interstrand cross-linked duplex concentration. (a) ICL-**44**; (b) ICL-**44** measured in a 1:1 (v/v) mixture of buffer (see above) and formamide; (c) ICL-**44** (2 μM); (d) ICL-**45**.

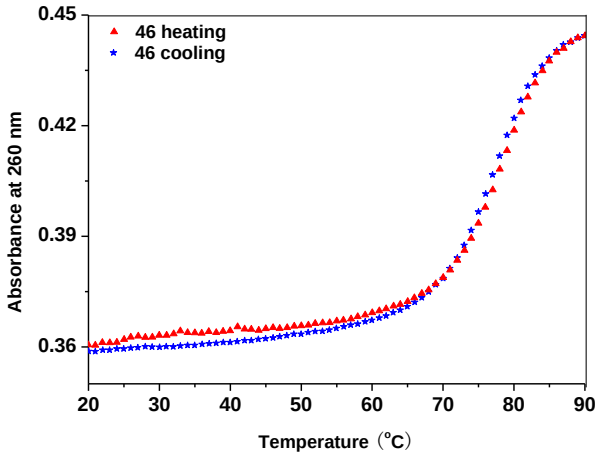

(a)

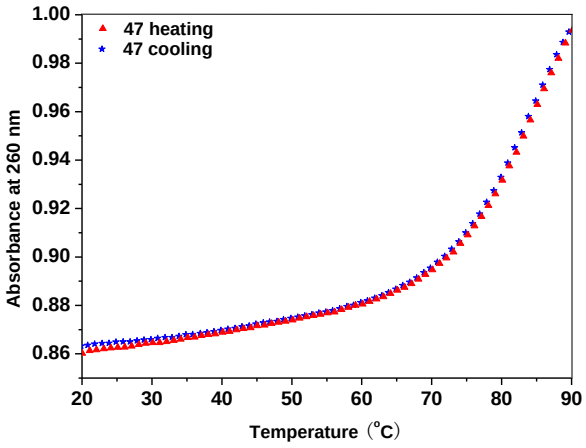

(b)

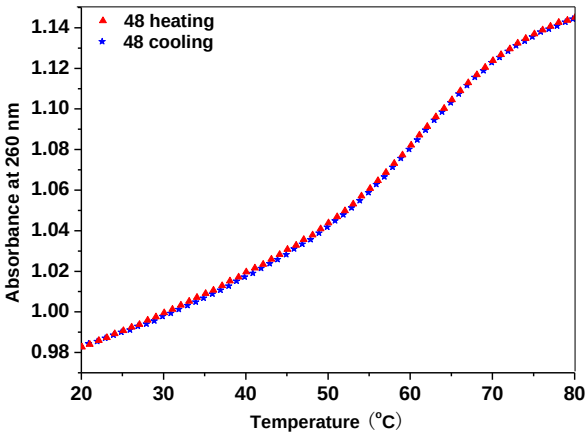

(c)

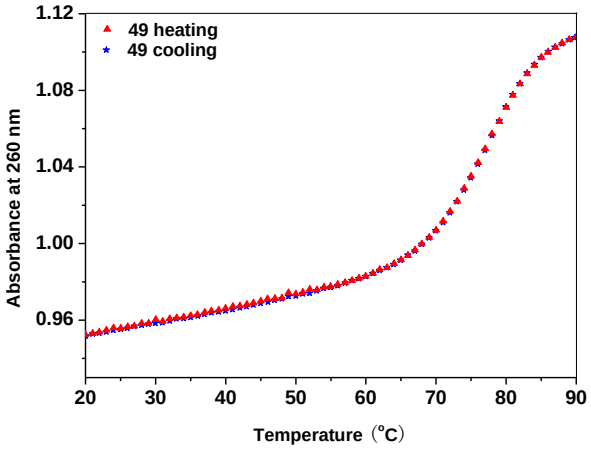

(d)

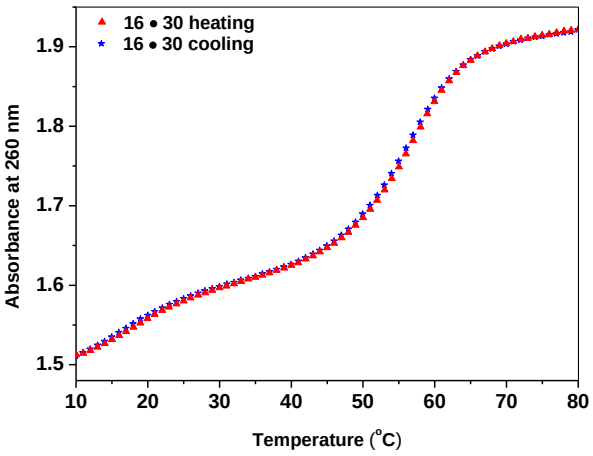

(e)

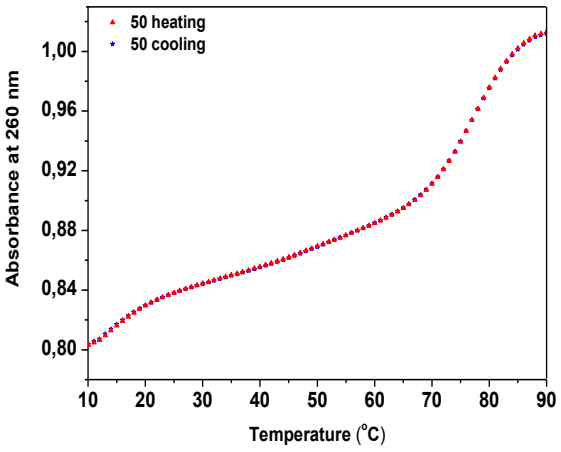

(f)

Figure S17. Original melting curves obtained from heating (red triangles) and cooling (blue stars) experiments measured at 260 nm in a 1 M NaCl solution containing 100 mM $MgCl_2$ and 60 mM Na-cacodylate (pH 7.0) with 5 μM of interstrand cross-linked duplex concentration. (a) ICL-**46** (2 μM); (b) ICL-**47**; (c) ICL-**48**; (d) ICL-**49**; (e) duplex **16•30** (5 μM + 5 μM); (f) ICL-**50**.

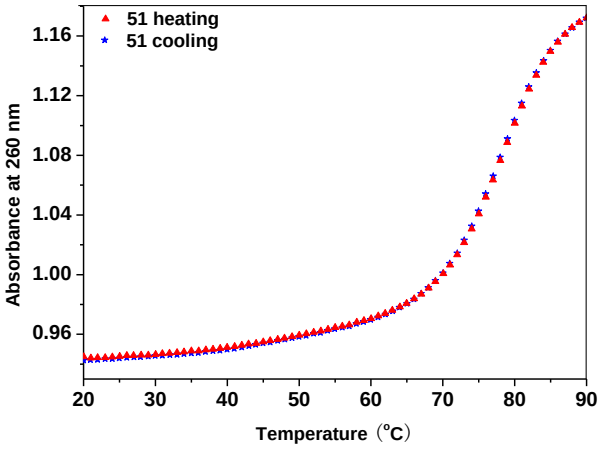

(a)

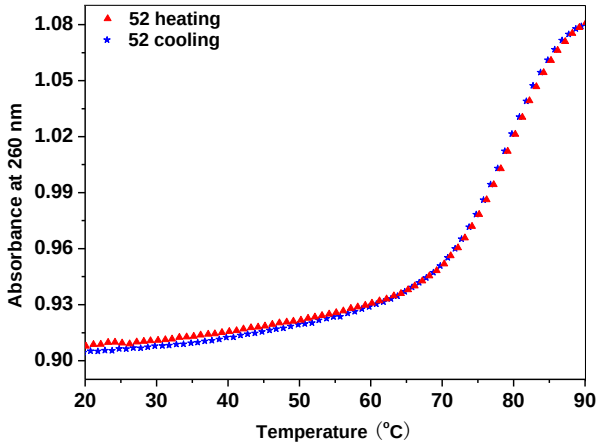

(b)

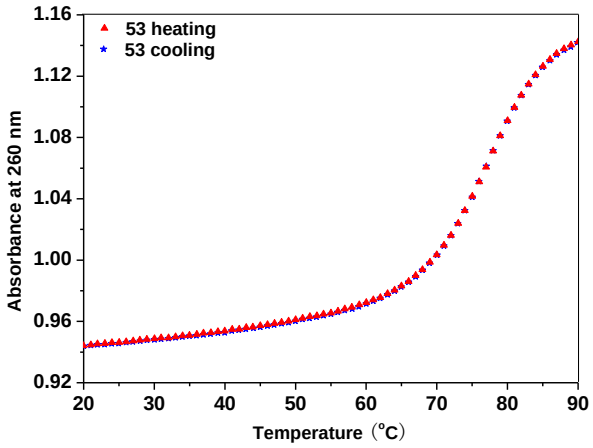

(c)

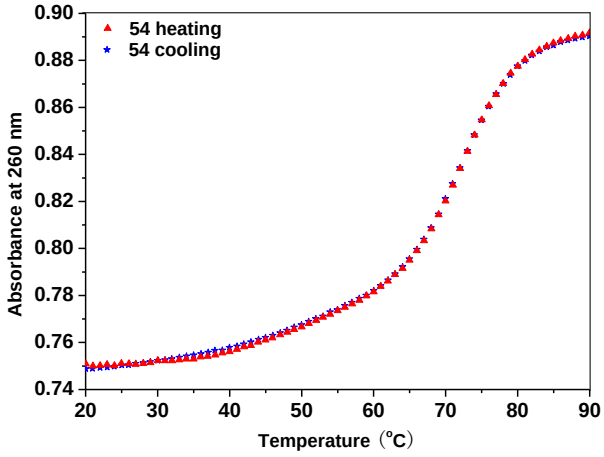

(d)

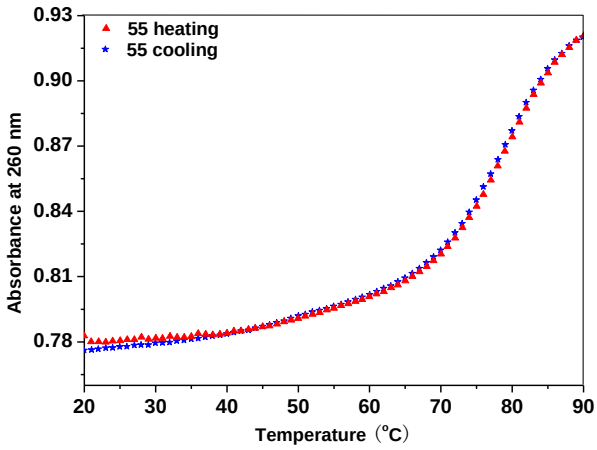

(e)

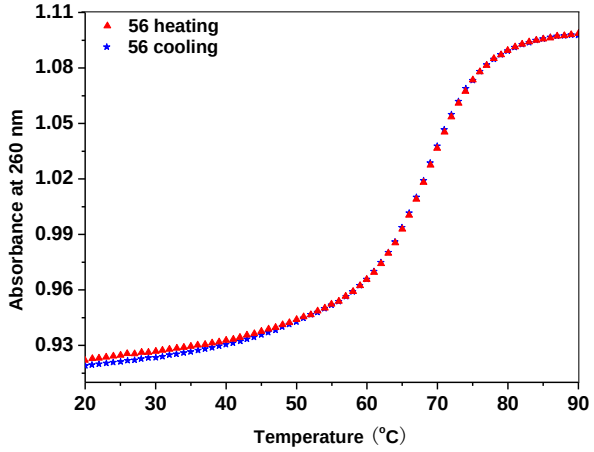

(f)

Figure S18. Original melting curves obtained from heating (red triangles) and cooling (blue stars) experiments measured at 260 nm in a 1 M NaCl solution containing 100 mM $MgCl_2$ and 60 mM Na-cacodylate (pH 7.0) with 5 μM of interstrand cross-linked duplex concentration. (a) to (f) ICL-**51** to ICL-**56**.

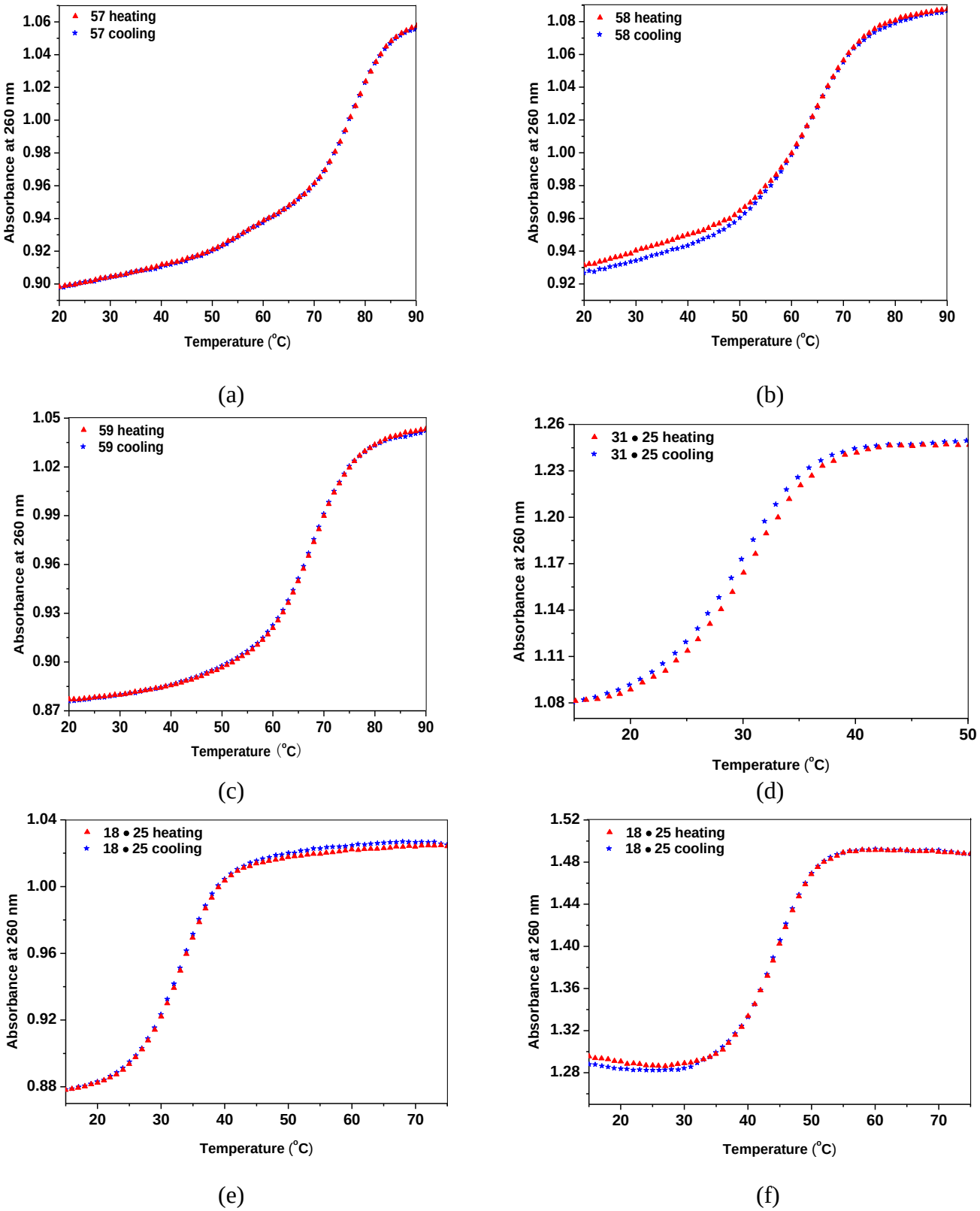

Figure S19. Original melting curves obtained from heating (red triangles) and cooling (blue stars) experiments measured at 260 nm in a 1 M NaCl solution containing 100 mM $MgCl_2$ and 60 mM Na-cacodylate (pH 7.0) with 5 μM of interstrand cross-linked duplex concentration. (a) to (c) ICL-**57** to ICL-**59**; (d) duplex **31•25** measured in 40 mM of $NaHCO_3$ containing 6 vol% *t*-BuOH; (e) duplex **18•25** measured in 40 mM of $NaHCO_3$ containing 6 vol% *t*-BuOH; (f) duplex **18•25** measured in 0.4 M of NaCl containing 40 mM of $NaHCO_3$. (d) to (f), 5 μM + 5 μM single-strand concentration.

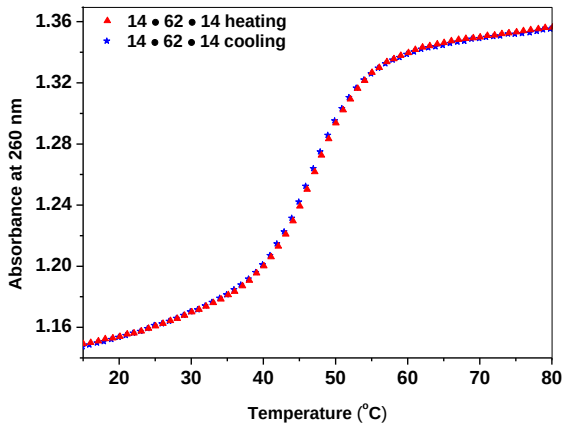

(a)

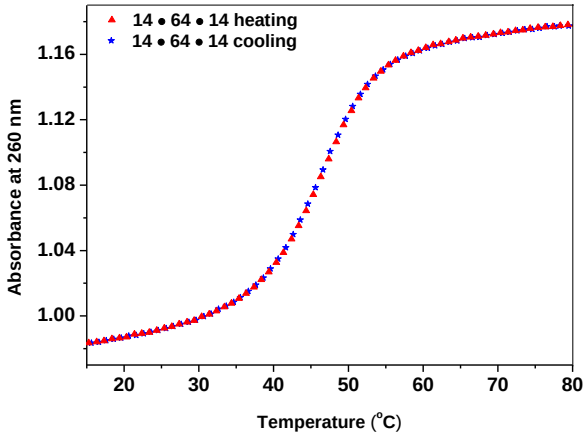

(b)

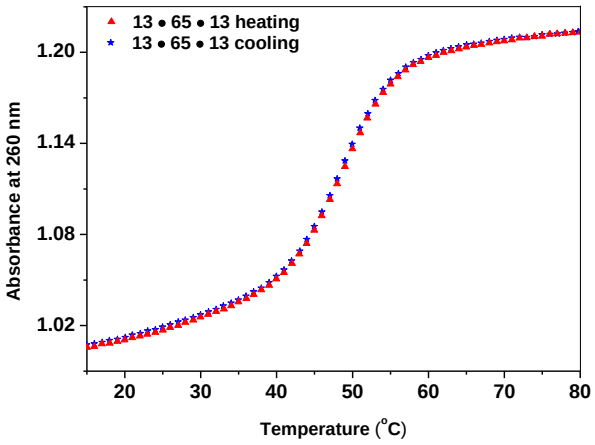

(c)

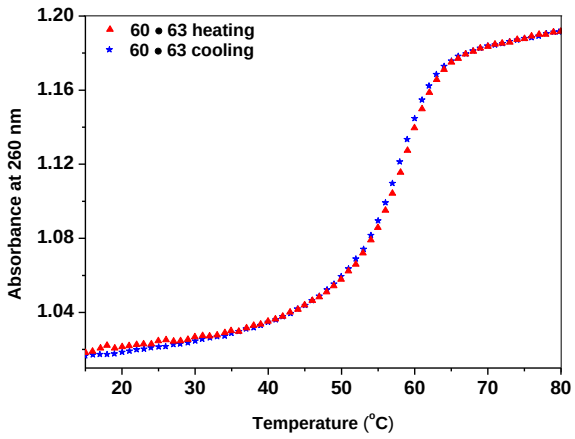

(d)

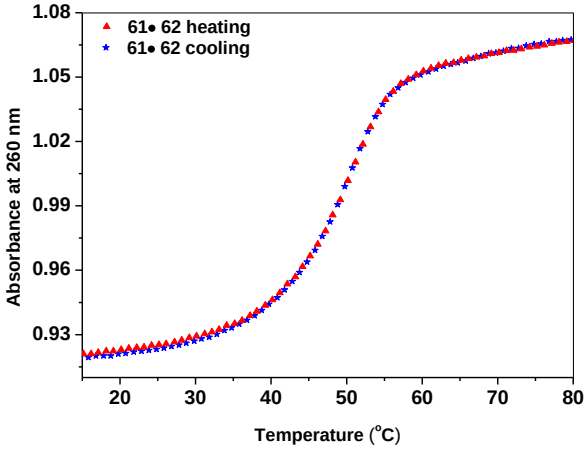

(e)

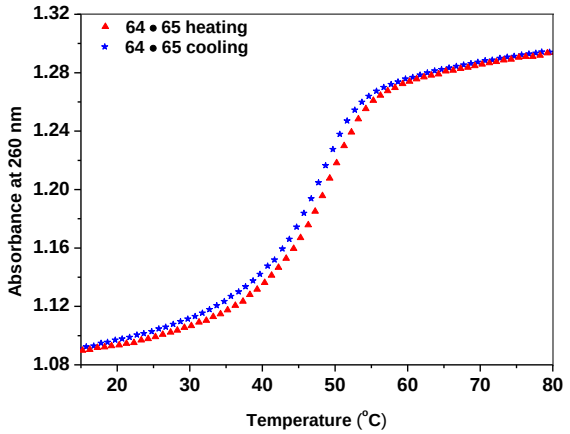

(f)

Figure S20. Original melting curves obtained from heating (red triangles) and cooling (blue stars) experiments measured at 260 nm in a 1 M NaCl solution containing 100 mM $MgCl_2$ and 60 mM Na-cacodylate (pH 7.0) with 2.5 μM of the interstrand cross-linked oligonucleotide and 5 μM of the complementary oligonucleotide (a) to (c): (a) duplex **14•62•14**; (b) duplex **14•64•14**; (c) duplex **13•65•13**. For (d) to (f): (d) duplex **60•63**; (e) duplex **61•62** and (f) duplex **64•65** with 2.5 μM + 2.5 μM of the interstrand cross-linked oligonucleotides.

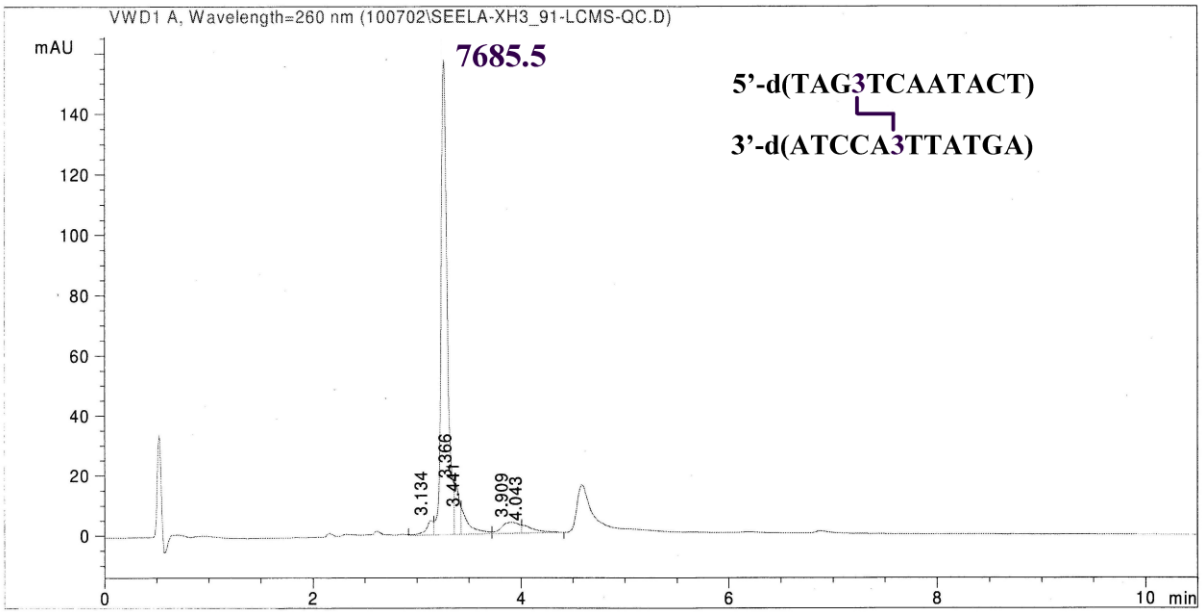

Figure S21. LC-ESI-MS chromatogram of ICL-**39**.

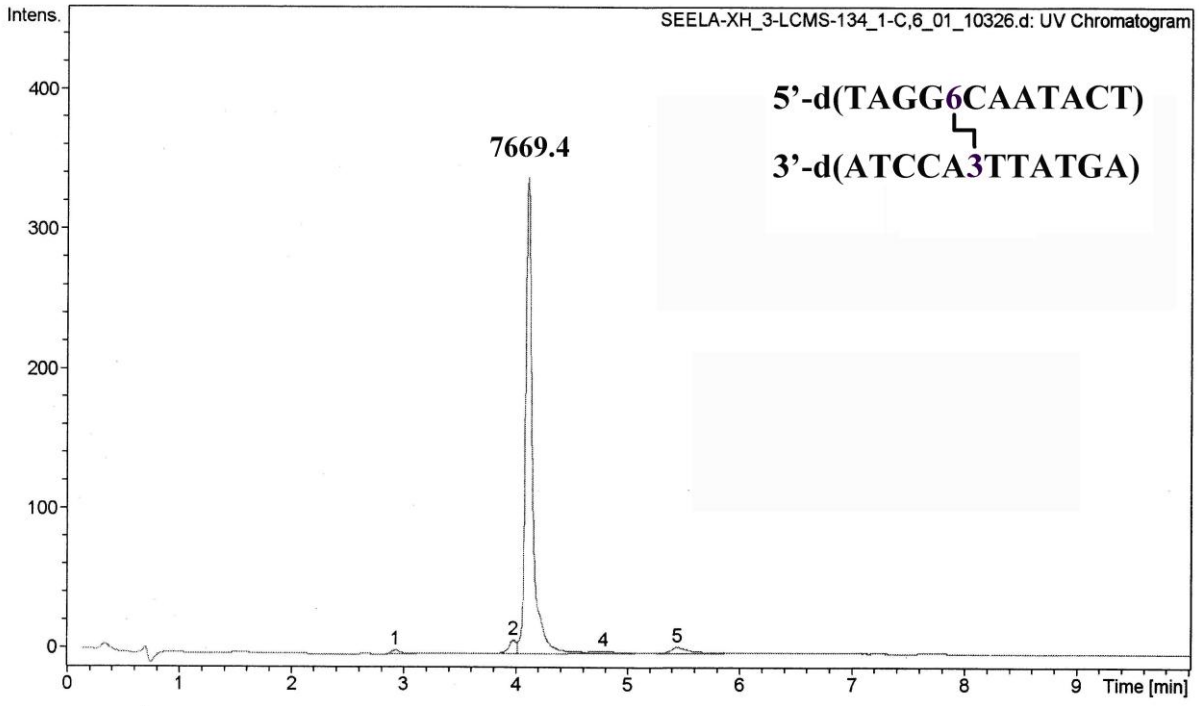

Figure S22. LC-ESI-MS chromatogram of ICL-**40**.

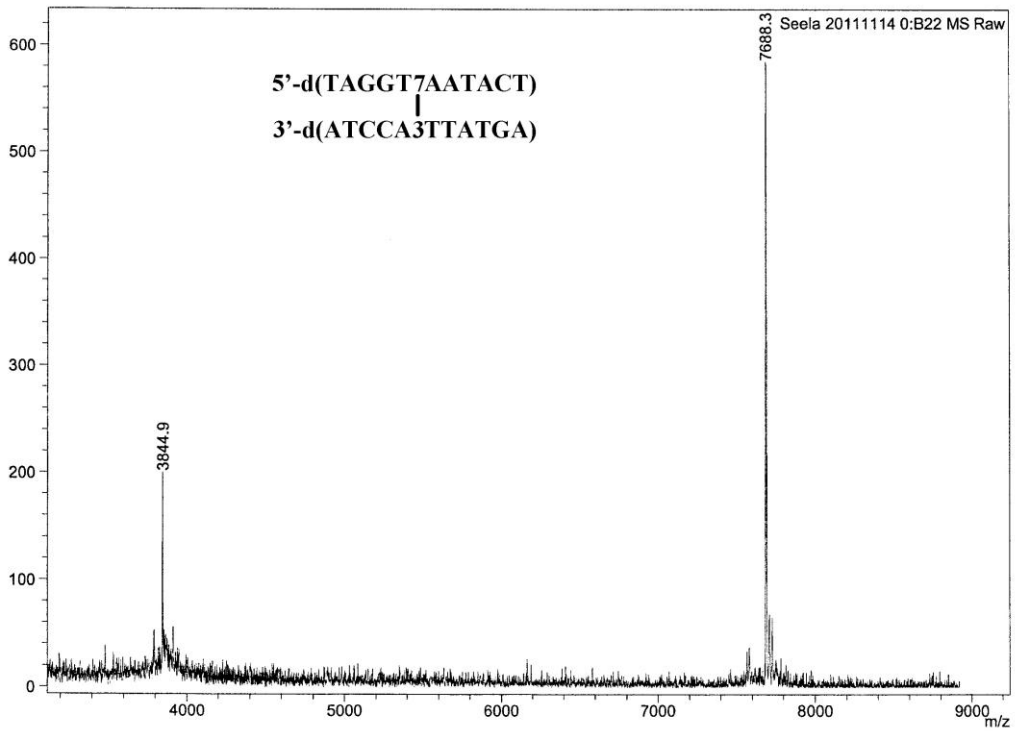

Figure S23. MALDI-TOF mass spectrum of ICL-**41**.

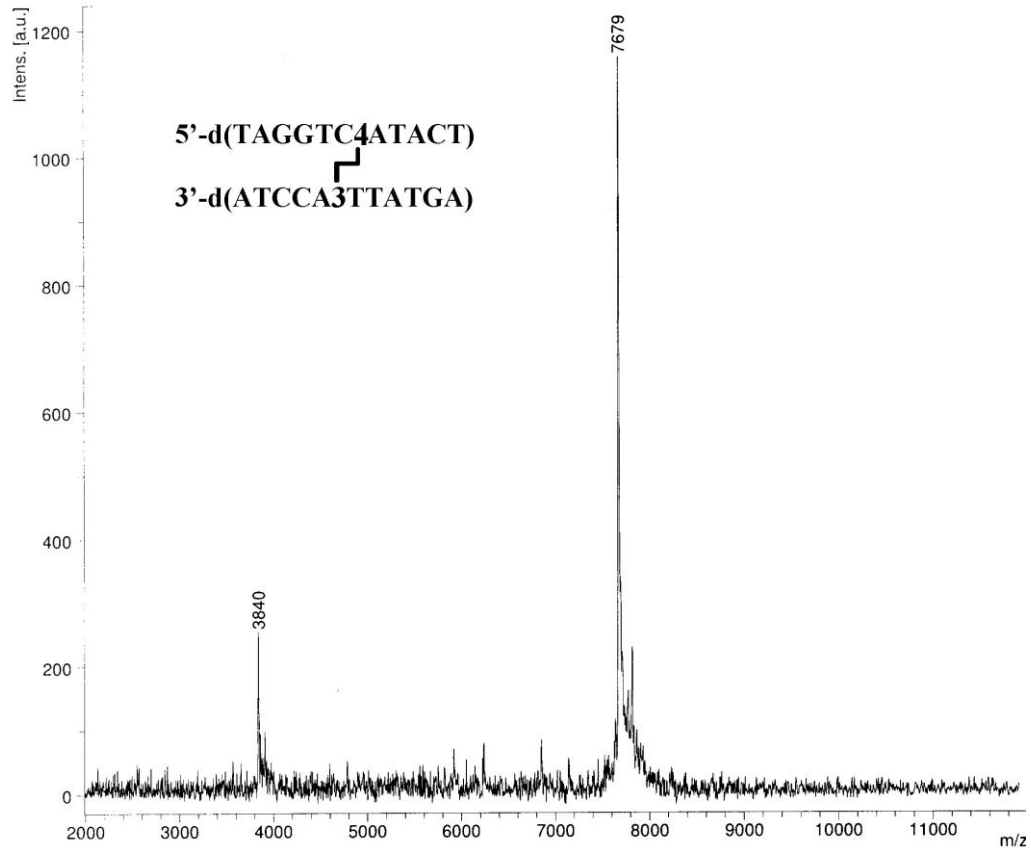

Figure S24. MALDI-TOF mass spectrum of ICL-**42**.

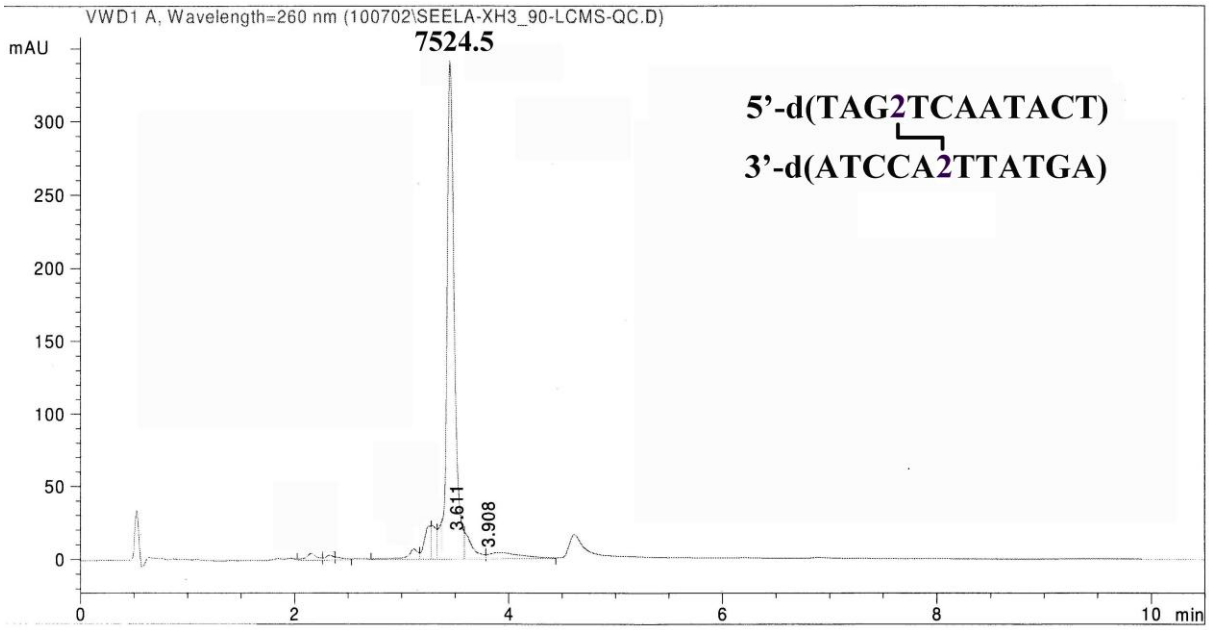

Figure S25. LC-ESI-MS chromatogram of ICL-**43**.

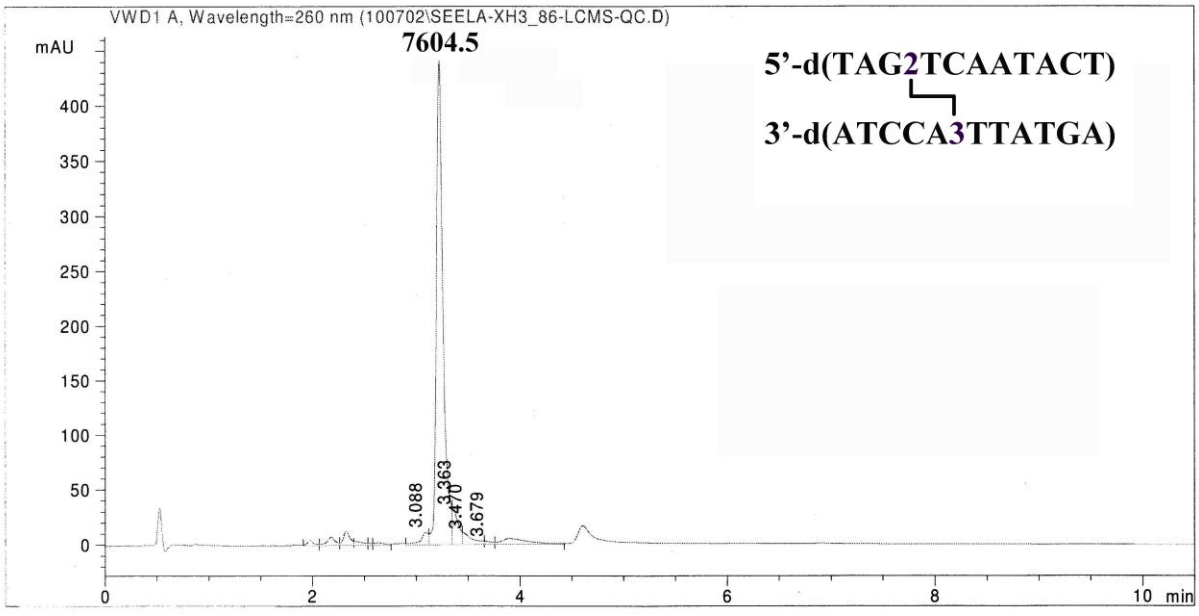

Figure S26. LC-ESI-MS chromatogram of ICL-**44**.

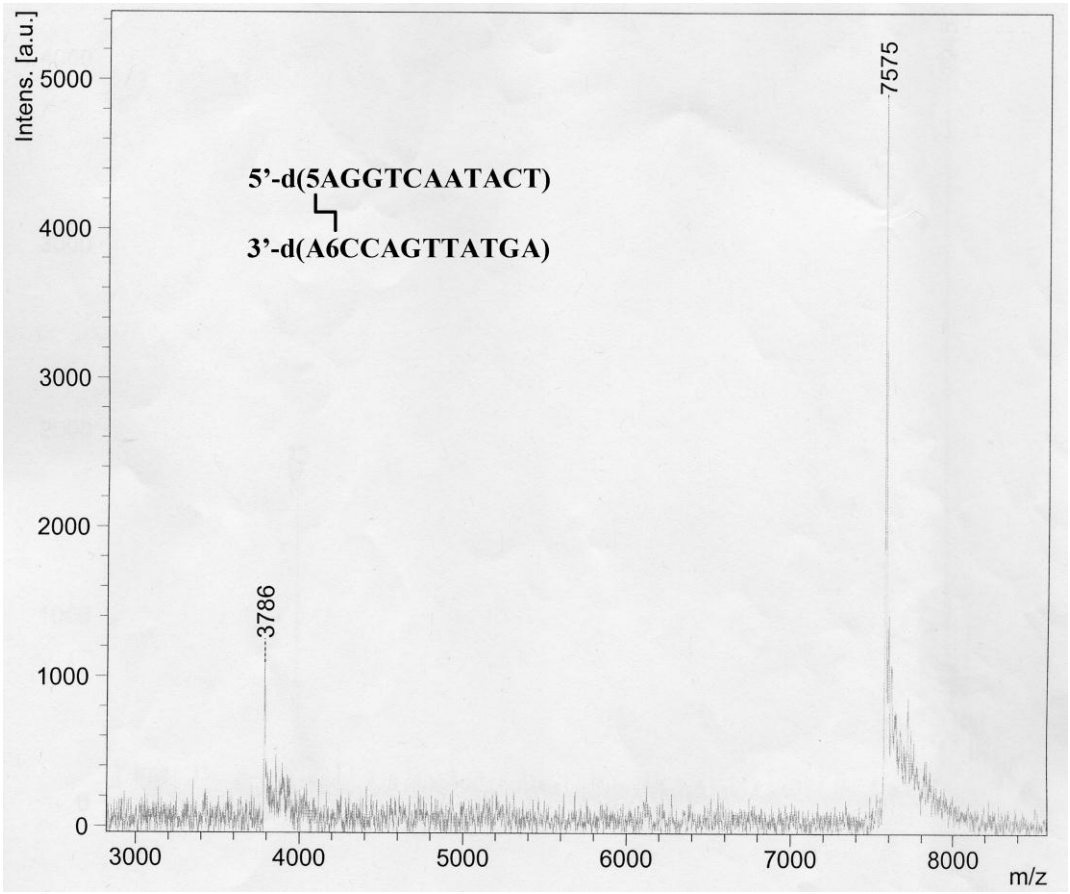

Figure S27. MALDI-TOF mass spectrum of ICL-**46**.

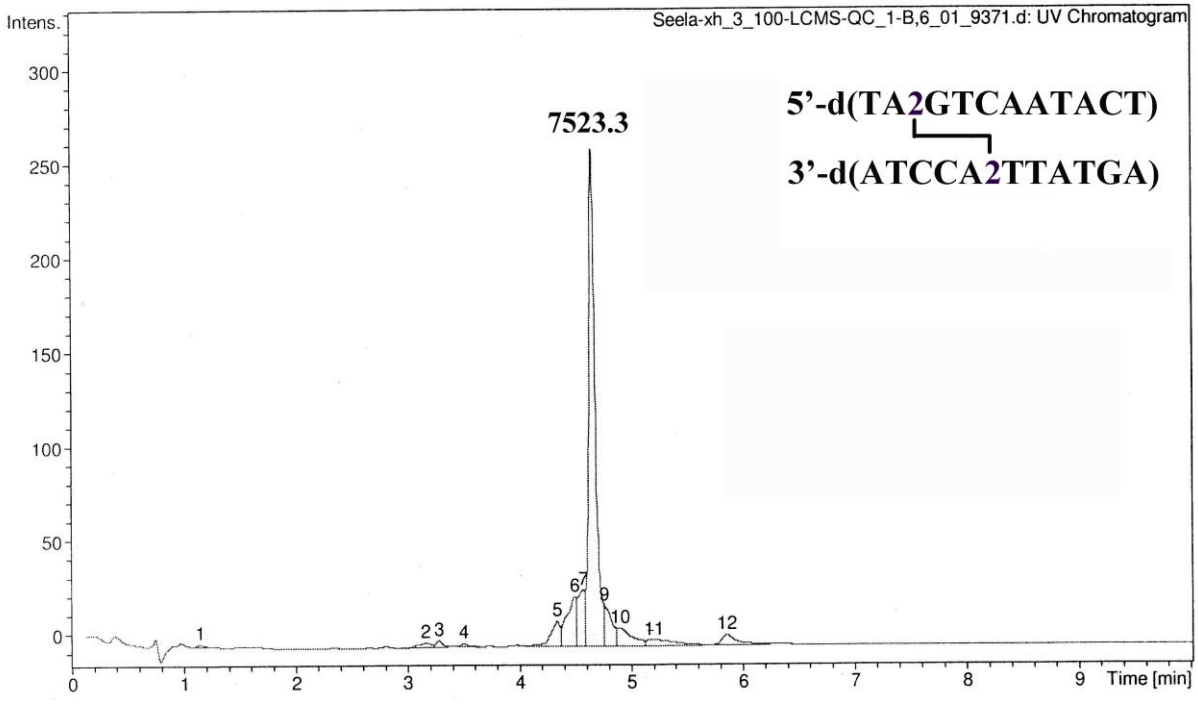

Figure S28. LC-ESI-MS chromatogram of ICL-**47**.

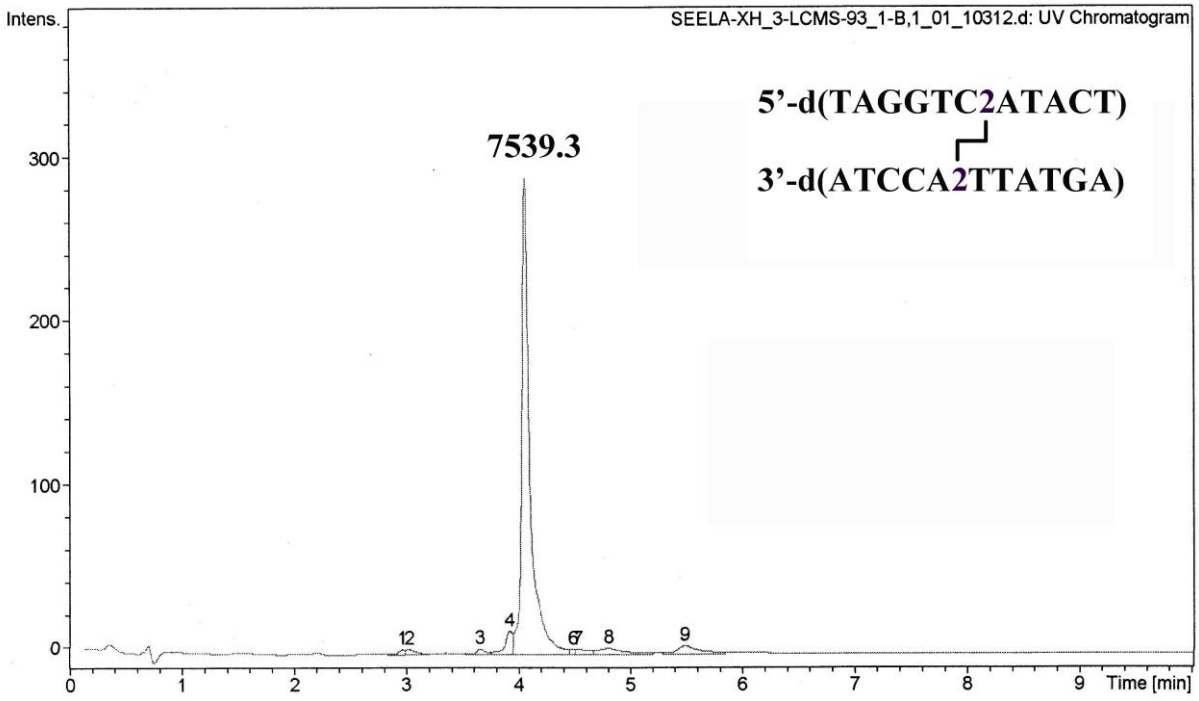

Figure S29. LC-ESI-MS chromatogram of ICL-**48**.

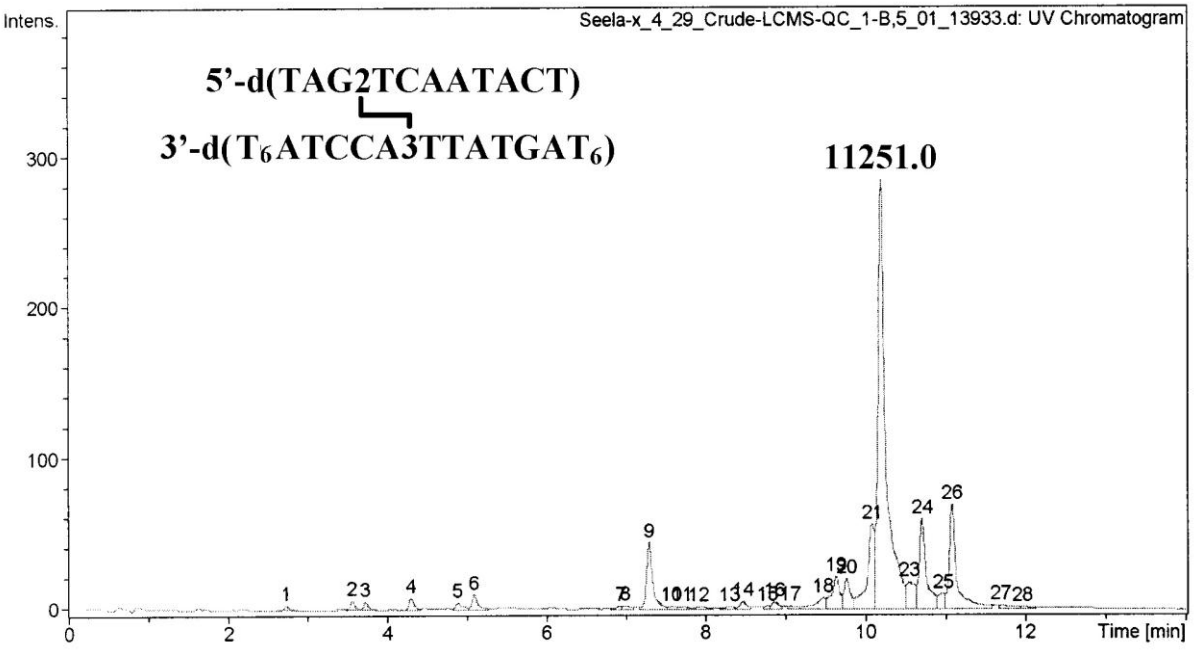

Figure S30. LC-ESI-MS chromatogram of ICL-**49** (crude).

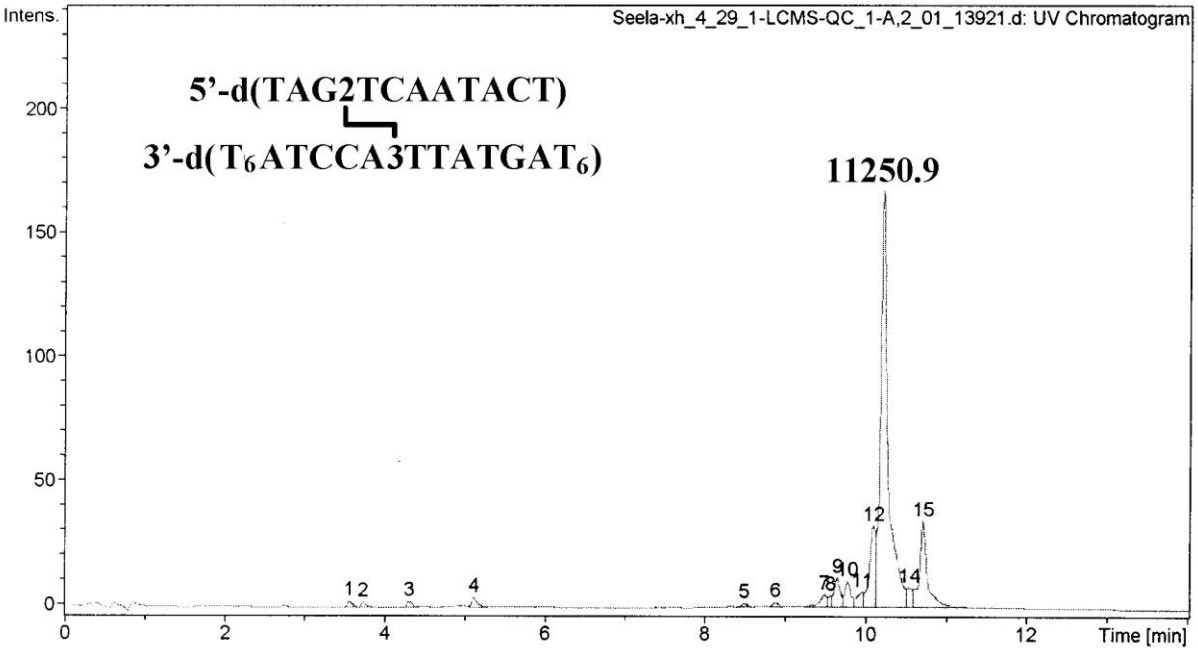

Figure S31. LC-ESI-MS chromatogram of ICL-**49**.

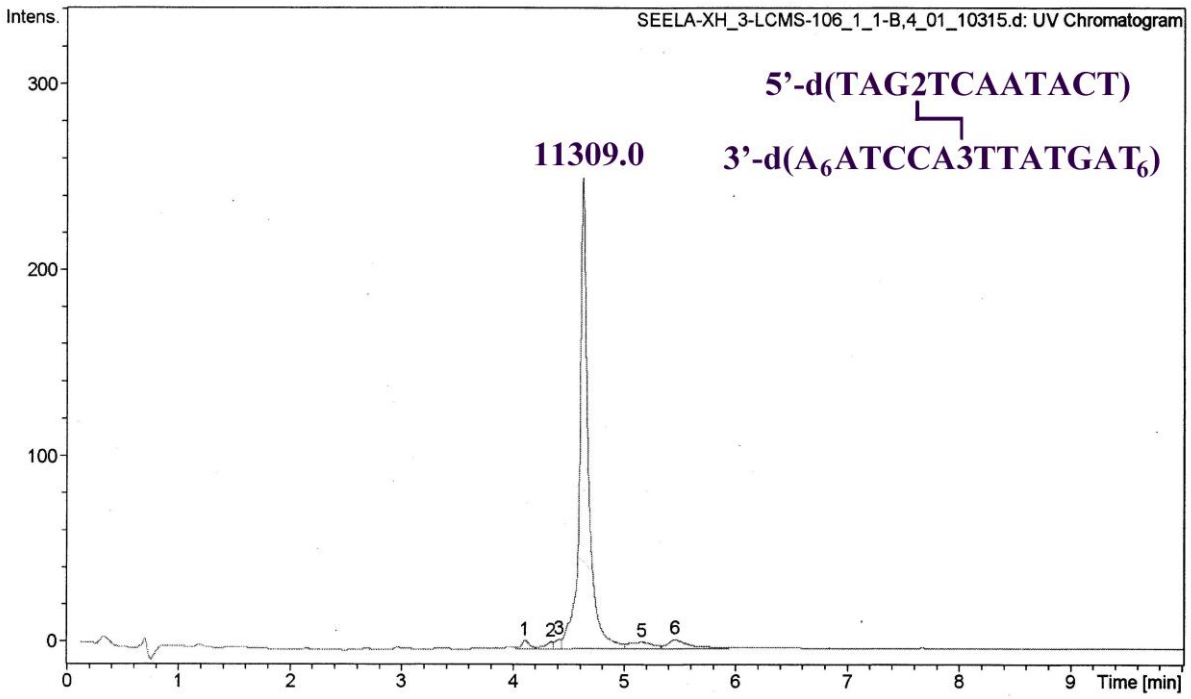

Figure S32. LC-ESI-MS chromatogram of ICL-**50**.

Figure S33. MALDI-TOF mass spectrum of ICL-**51**.

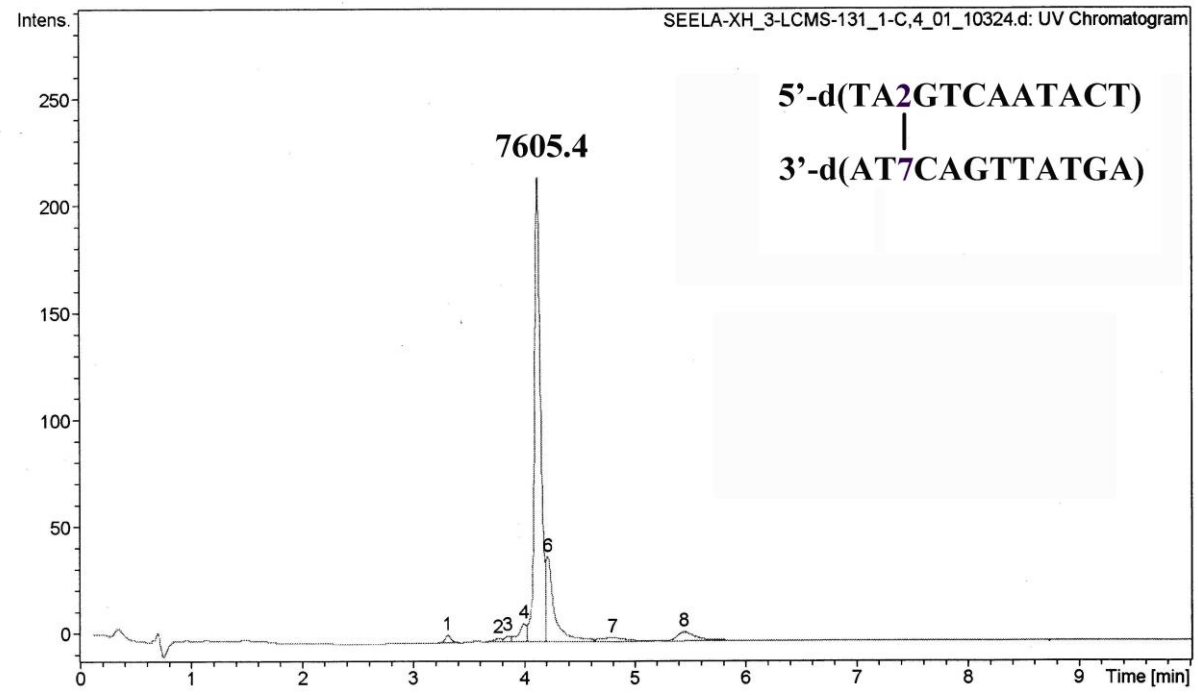

Figure S34. LC-ESI-MS chromatogram of ICL-**52**.

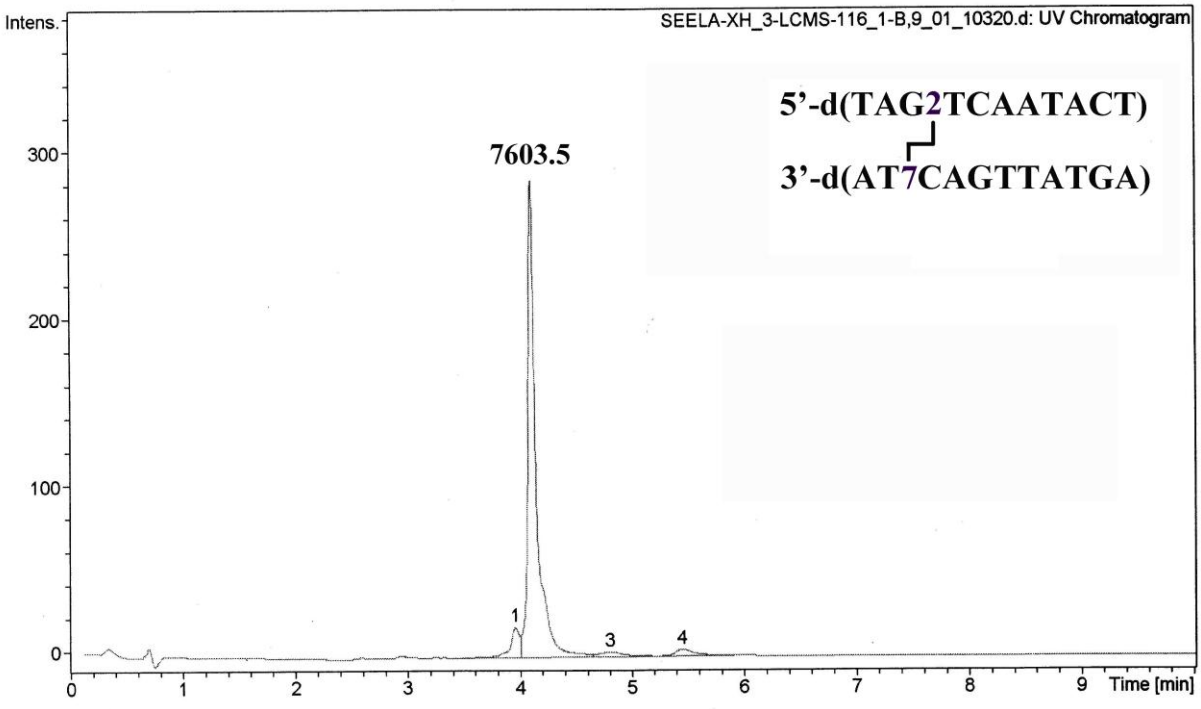

Figure S35. LC-ESI-MS chromatogram of ICL-**53**.

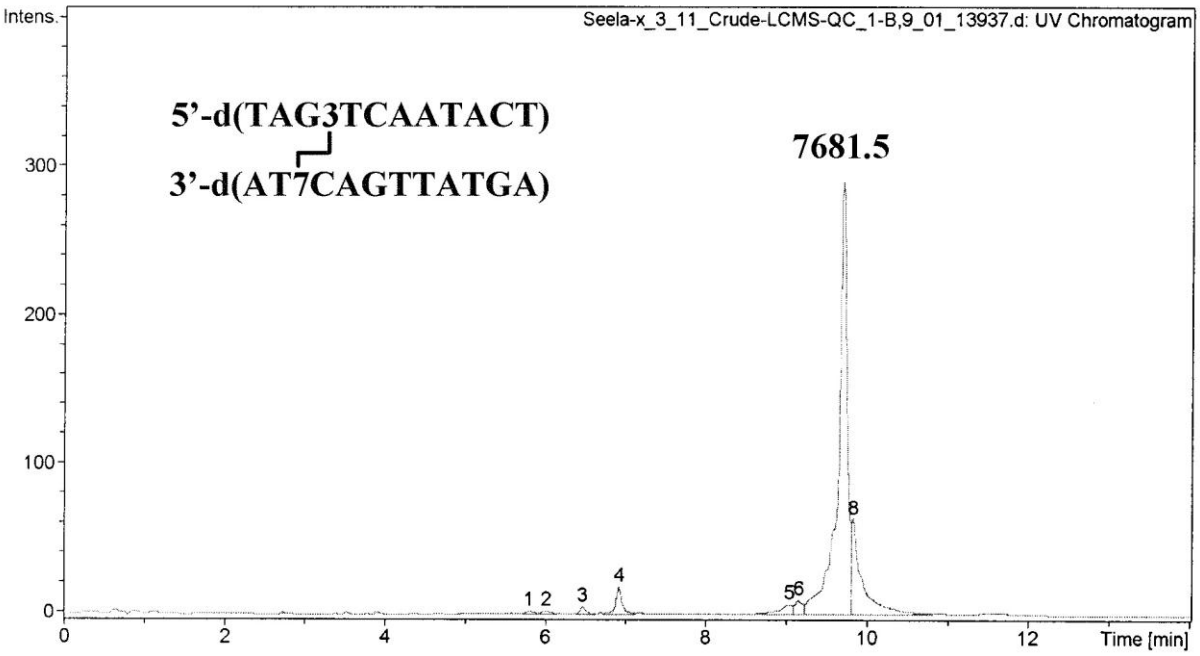

Figure S36. LC-ESI-MS chromatogram of ICL-**54** (crude).

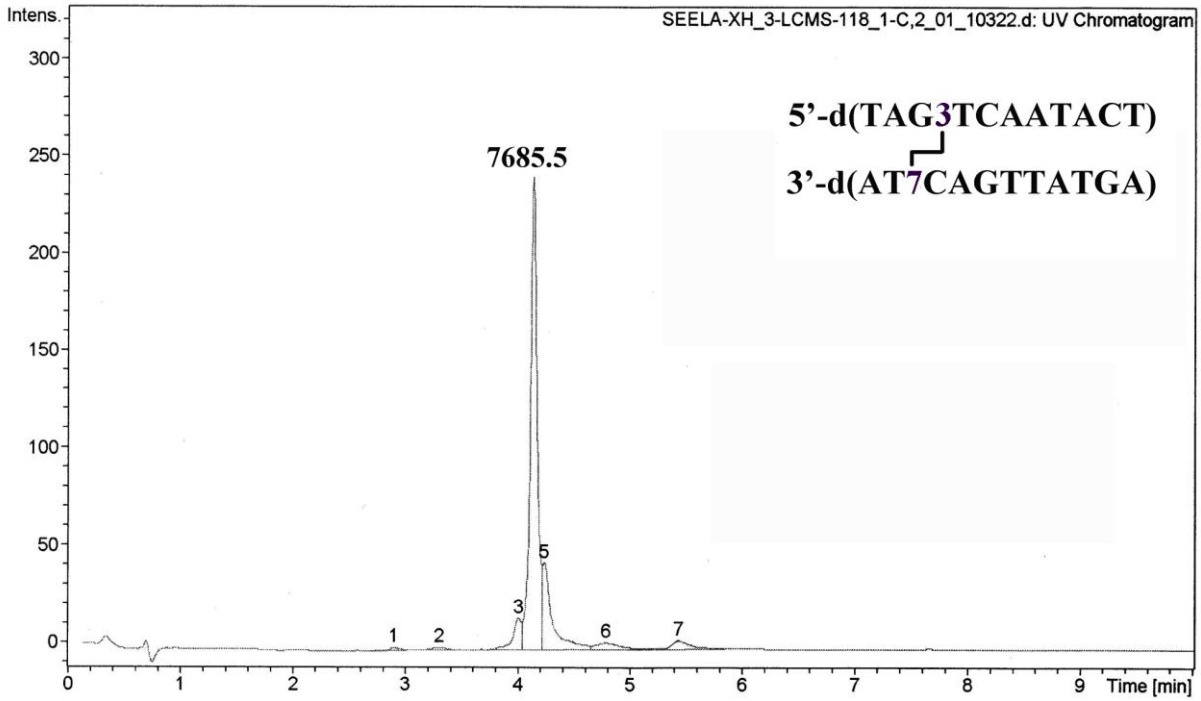

Figure S37. LC-ESI-MS chromatogram of ICL-**54**.

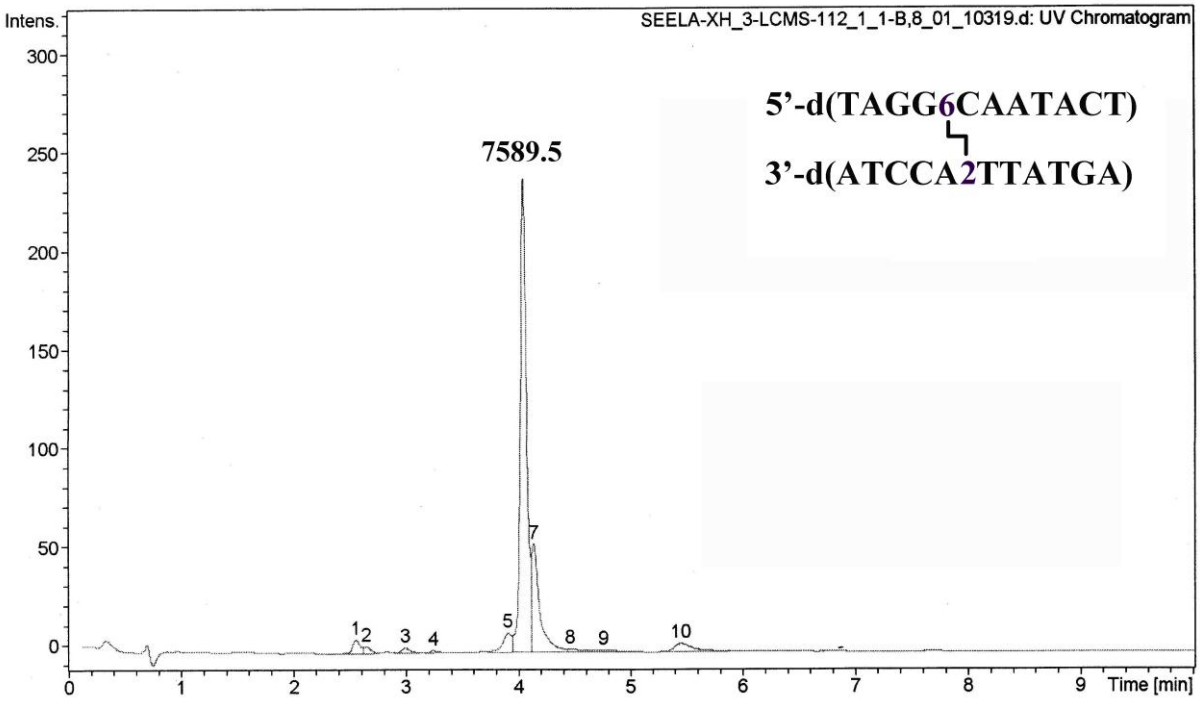

Figure S38. LC-ESI-MS chromatogram of ICL-**55**.

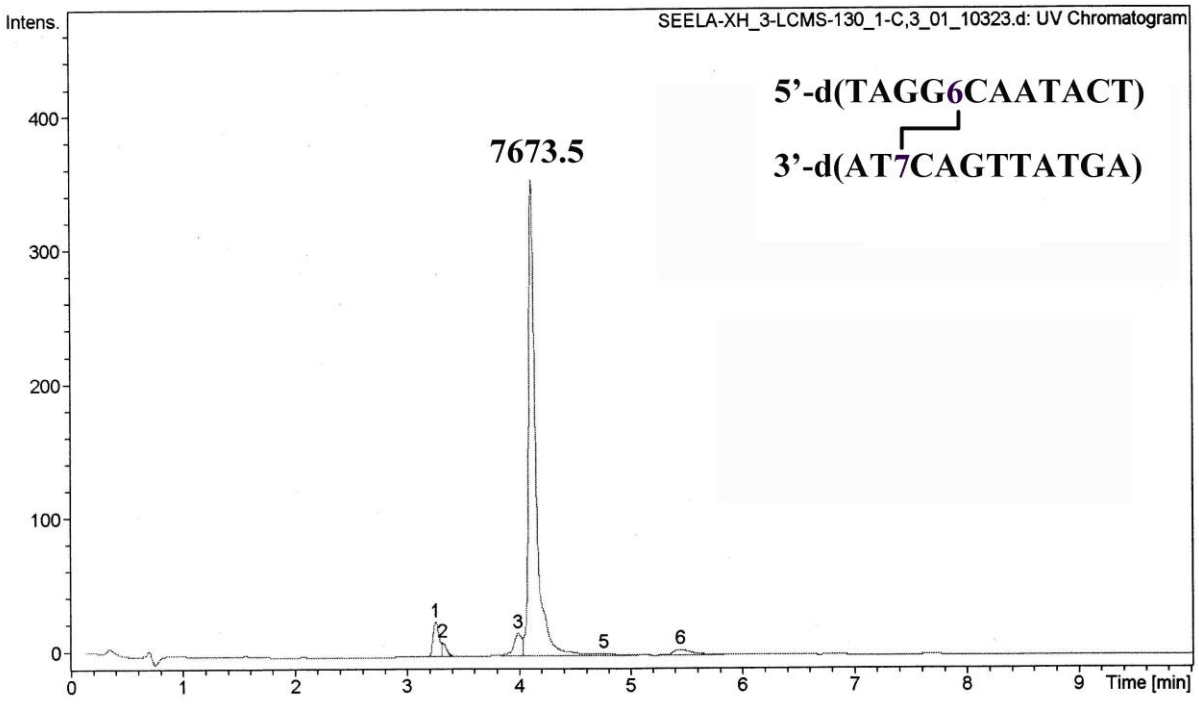

Figure S39. LC-ESI-MS chromatogram of ICL-**56**.

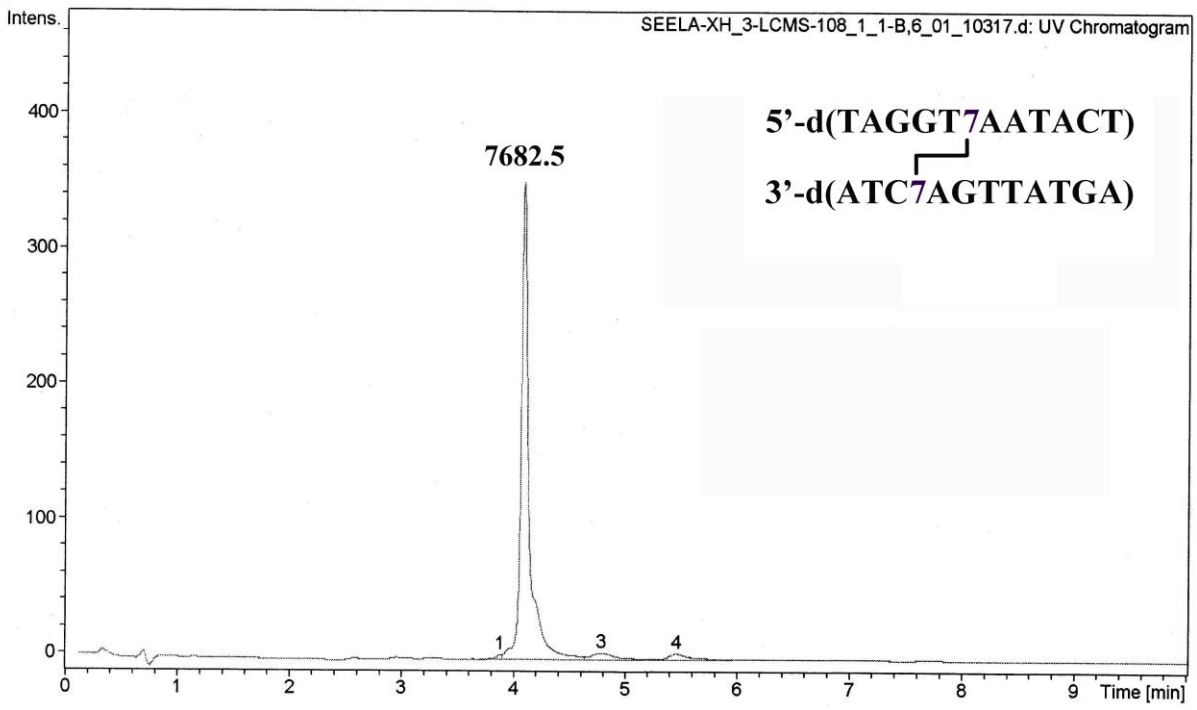

Figure S40. LC-ESI-MS chromatogram of ICL-**59**.

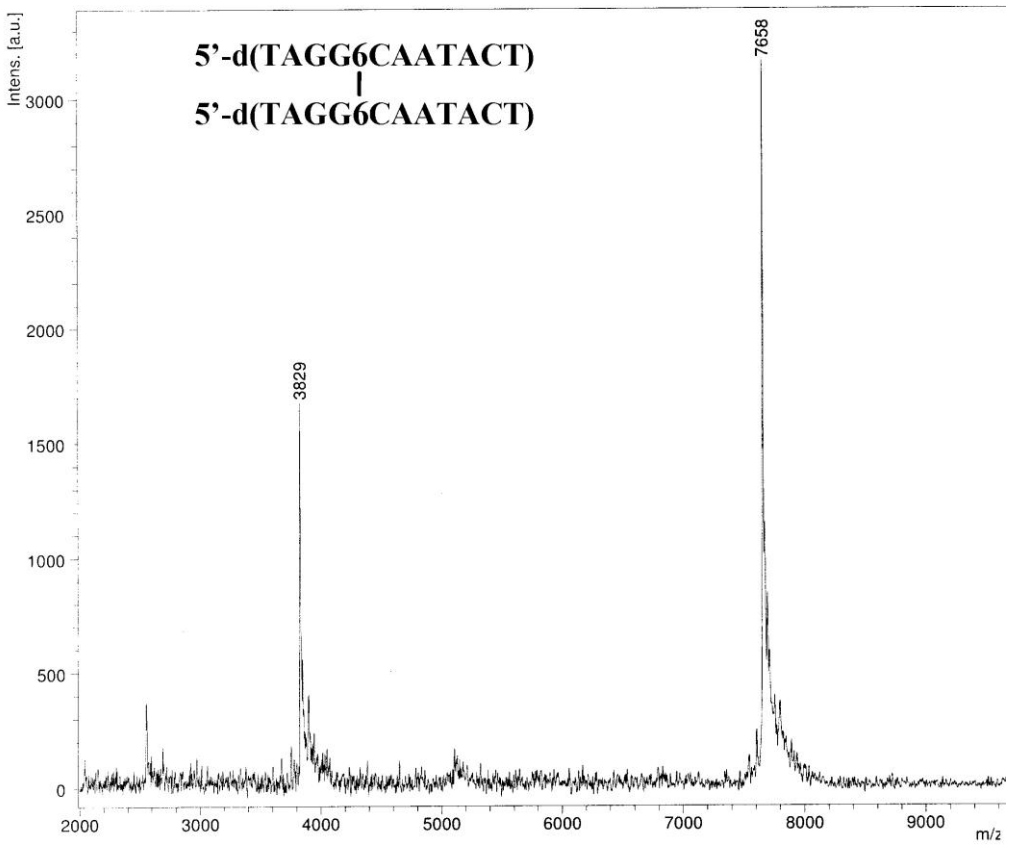

Figure S41. MALDI-TOF mass spectrum of ICL-**62**.

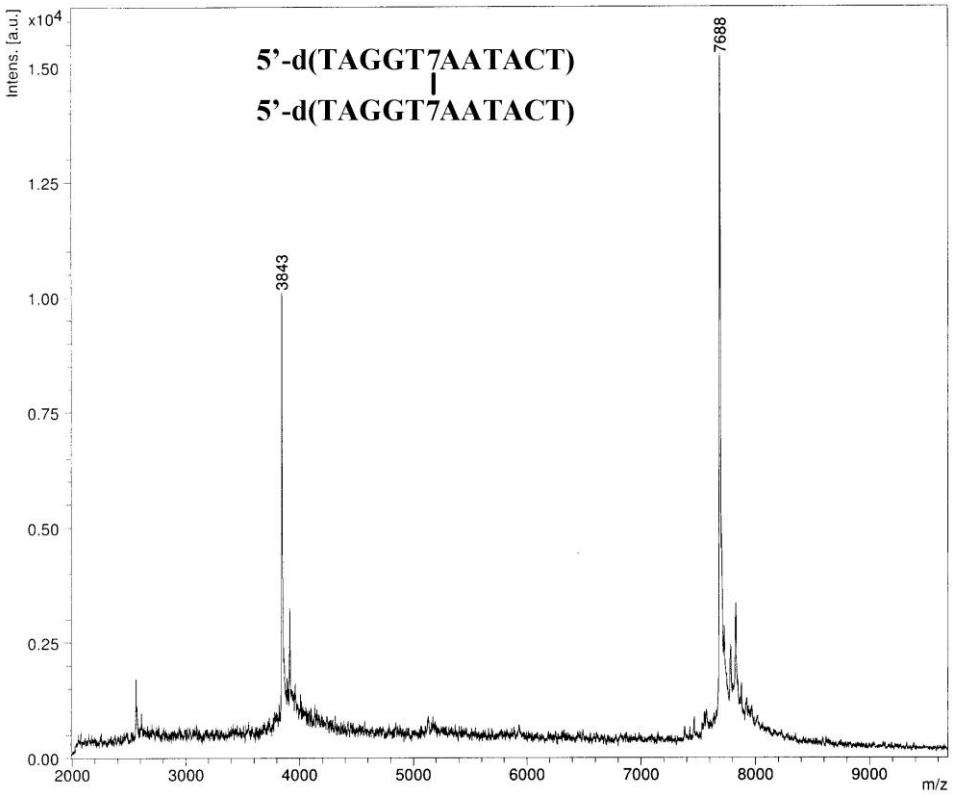

Figure S42. MALDI-TOF mass spectrum of ICL-**64**.

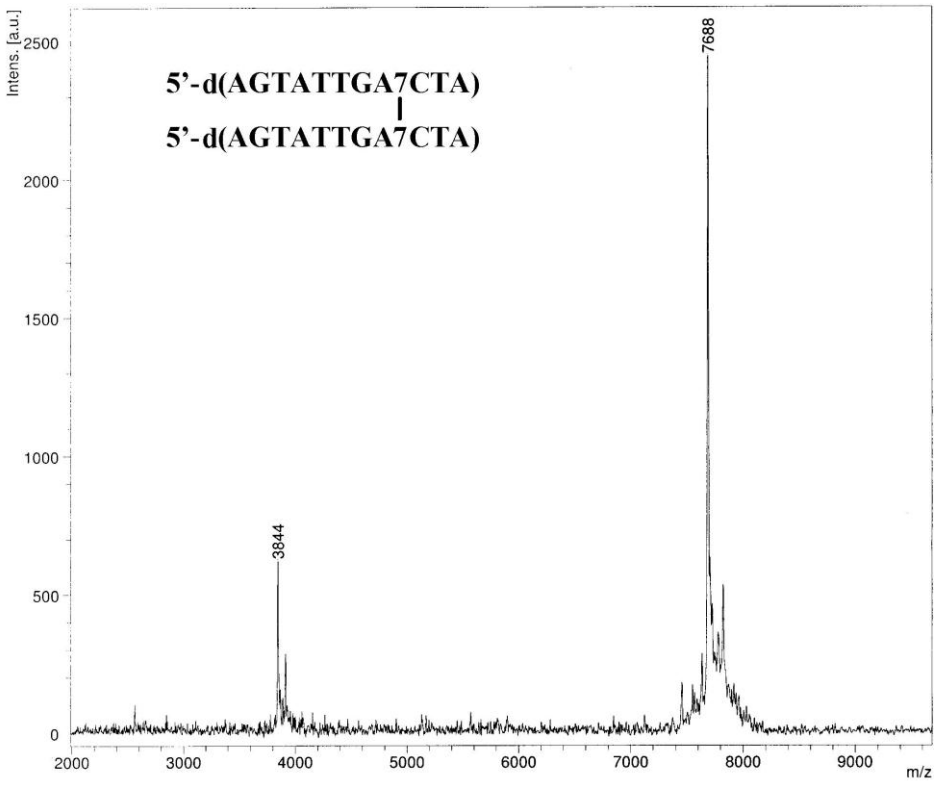

Figure S43. MALDI-TOF mass spectrum of ICL-**65**.

Table S5. Elemental Analysis of Nucleoside **10**.

Compound	Calculated			Found		
	C	H	N	C	H	N
10	57.68	5.42	21.53	57.80	5.40	21.30

LITERATURE CITED

(1) Seela, F., Xiong, H., Leonard, P., and Budow, S. (2009) 8-Aza-7-deazaguanine nucleosides and oligonucleotides with octadiynyl side chains: Synthesis, functionalization by the azide-alkyne ‘click’ reaction and nucleobase specific fluorescence quenching of coumarin dye conjugates. *Org. Biomol. Chem. 7*, 1374–1387.

(2) Graham, D.; Parkinson, J. A.; and Brown, T. (1998) DNA duplexes stabilized by modified monomer residues: Synthesis and stability. *J. Chem. Soc., Perkin Trans. 1* 1131–1138.

(3) Xiong, H., and Seela, F. (2011) Stepwise ”click” chemistry for the template independent construction of a broad variety of cross-linked oligonucleotides: Influence of linker length, position, and linking number on DNA duplex stability. *J. Org. Chem. 76*, 5584-5597.

(4) Seela, F., Sirivolu, V. R., and Chittepu, P. (2008) Modification of DNA with octadiynyl side chains: synthesis, base pairing, and formation of fluorescent coumarin dye conjugates of four nucleobases by the alkyne-azide “click” reaction. *Bioconjugate Chem. 19*, 211–224.

(5) Seela, F., and Sirivolu, V. R. (2007) Nucleosides and oligonucleotides with diynyl side chains: Base pairing and functionalization of 2'-deoxyuridine derivatives by the copper(I)-catalyzed alkyne–azide ‘click’ cycloaddition. *Helv. Chim. Acta 90*, 535–552.

(6) Seela, F., and Pujari, S. S. (2010) Azide-alkyne “click” conjugation of 8-aza-7-deazaadenine-DNA: Synthesis, duplex stability, and fluorogenic dye labeling. *Bioconjugate Chem. 21*, 1629–1641.

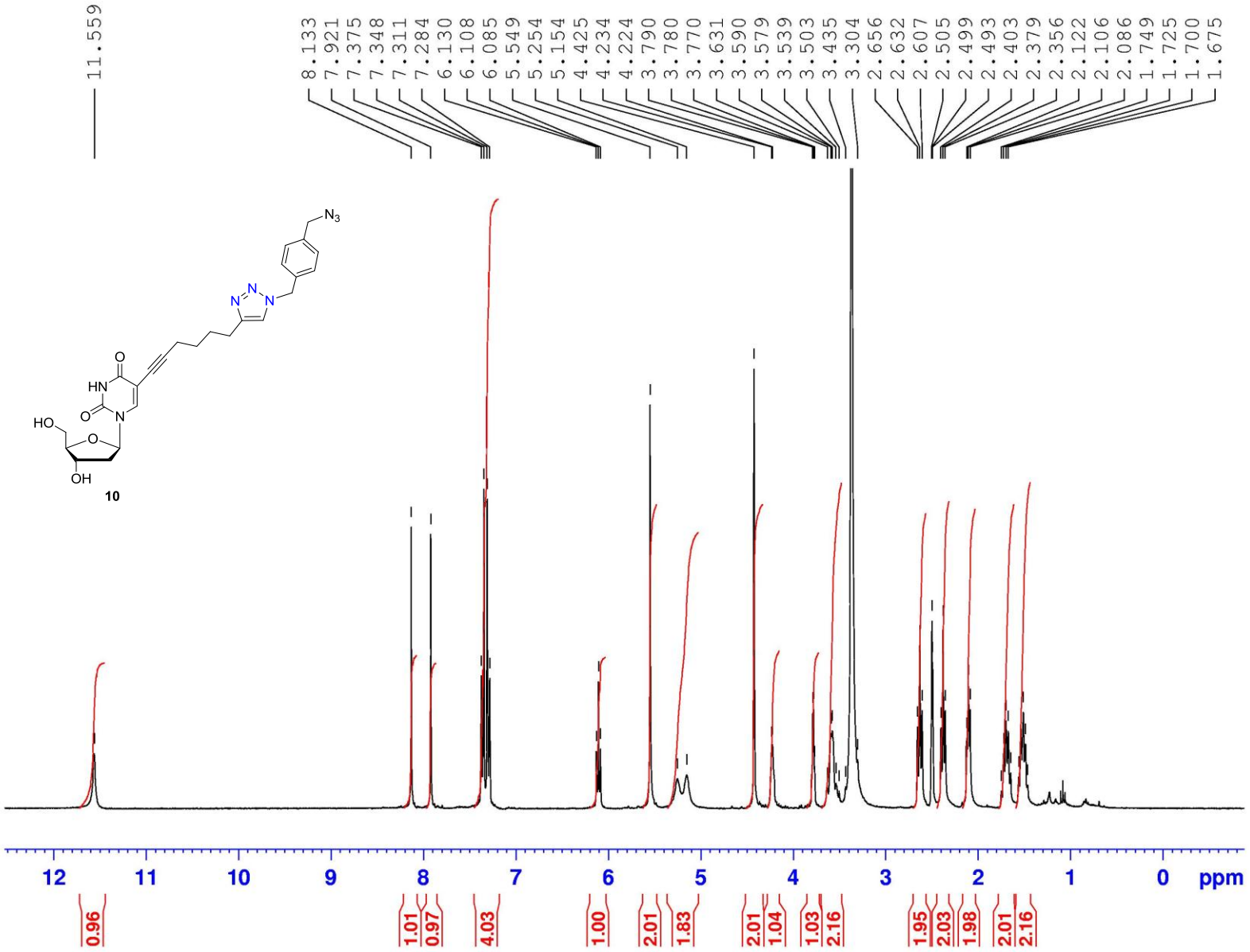

Figure S44. ^{1}H-NMR spectrum of compound **10**.

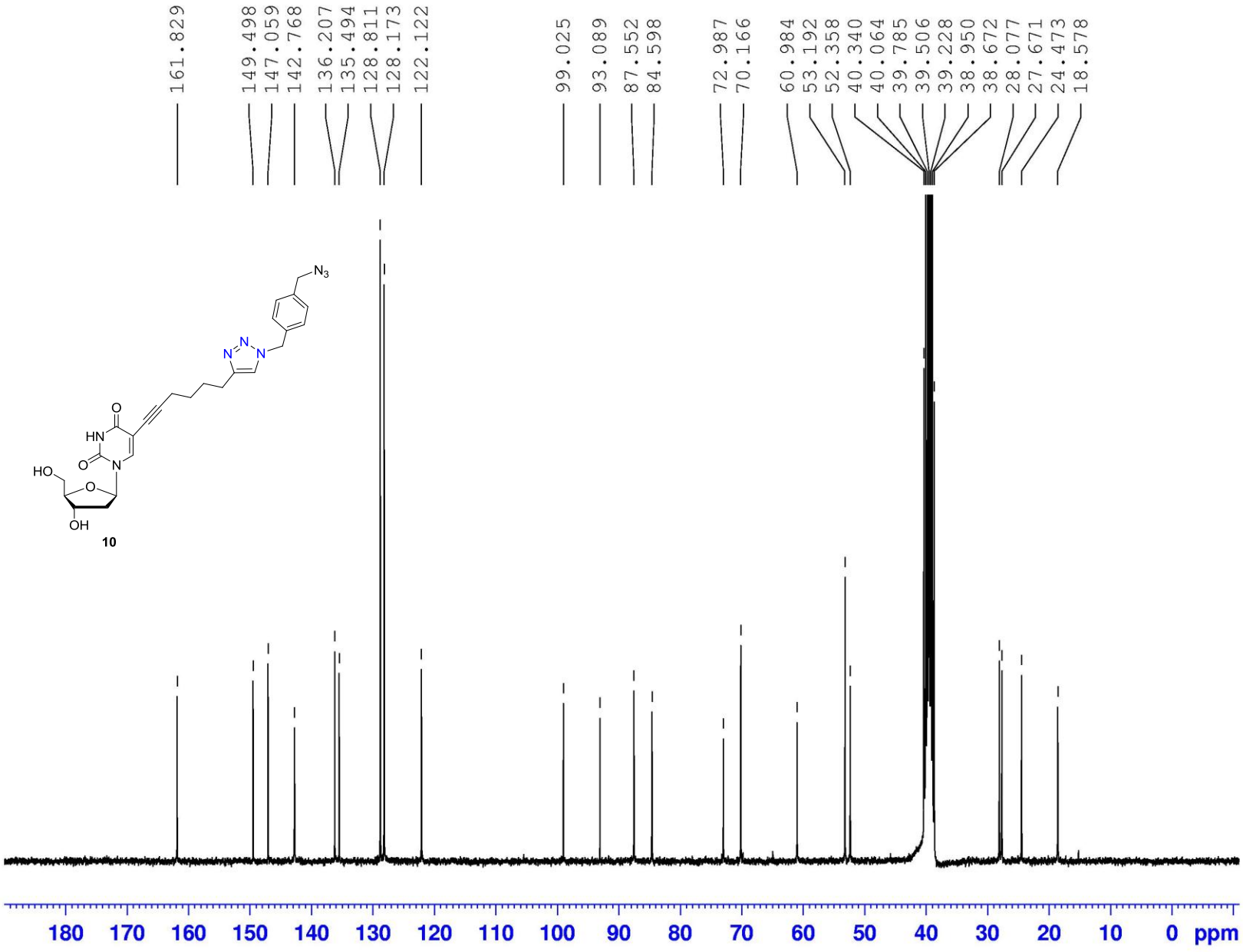

Figure S45. ^{13}C-NMR spectrum of compound **10**.

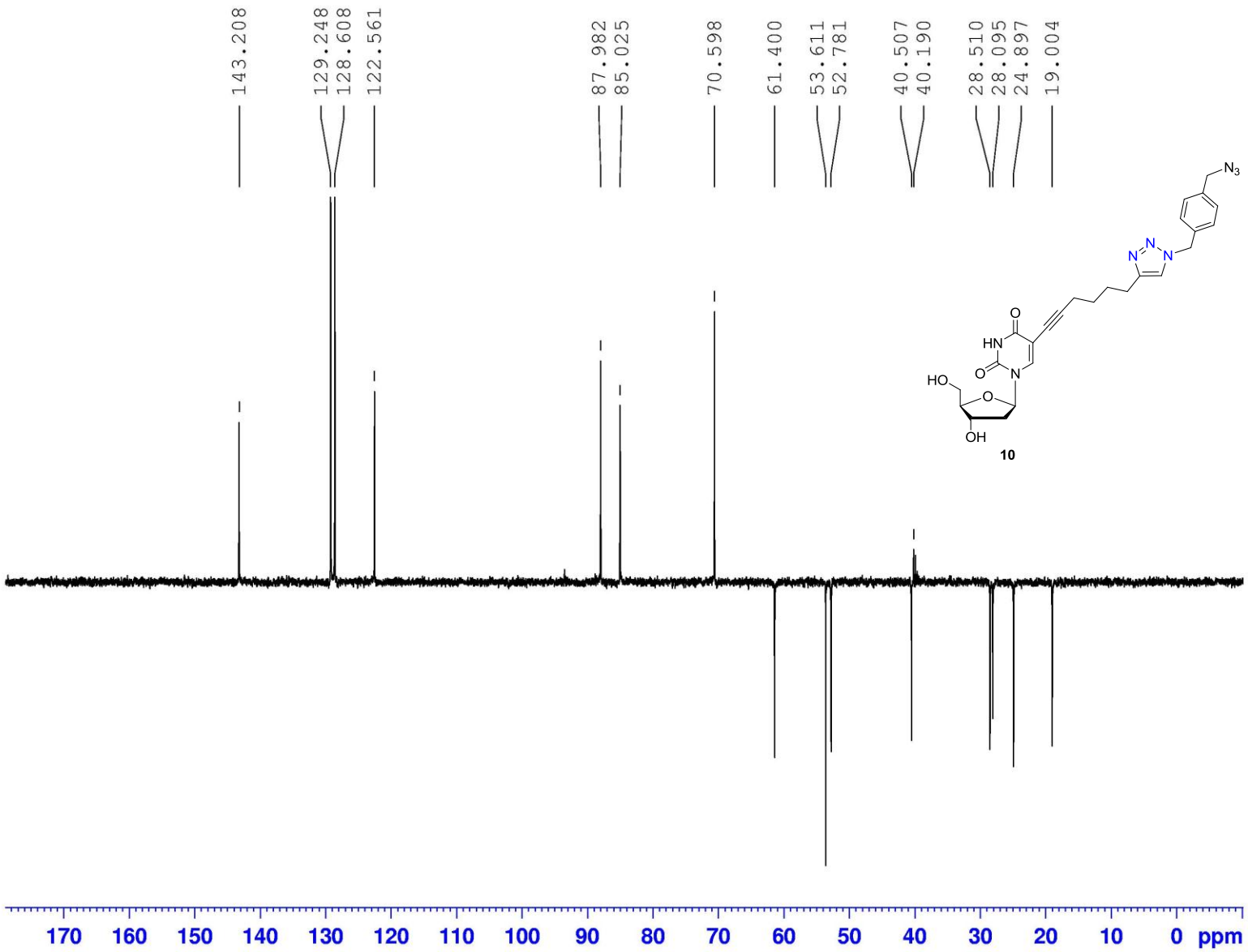

Figure S46. DEPT-135 spectrum of compound **10**.

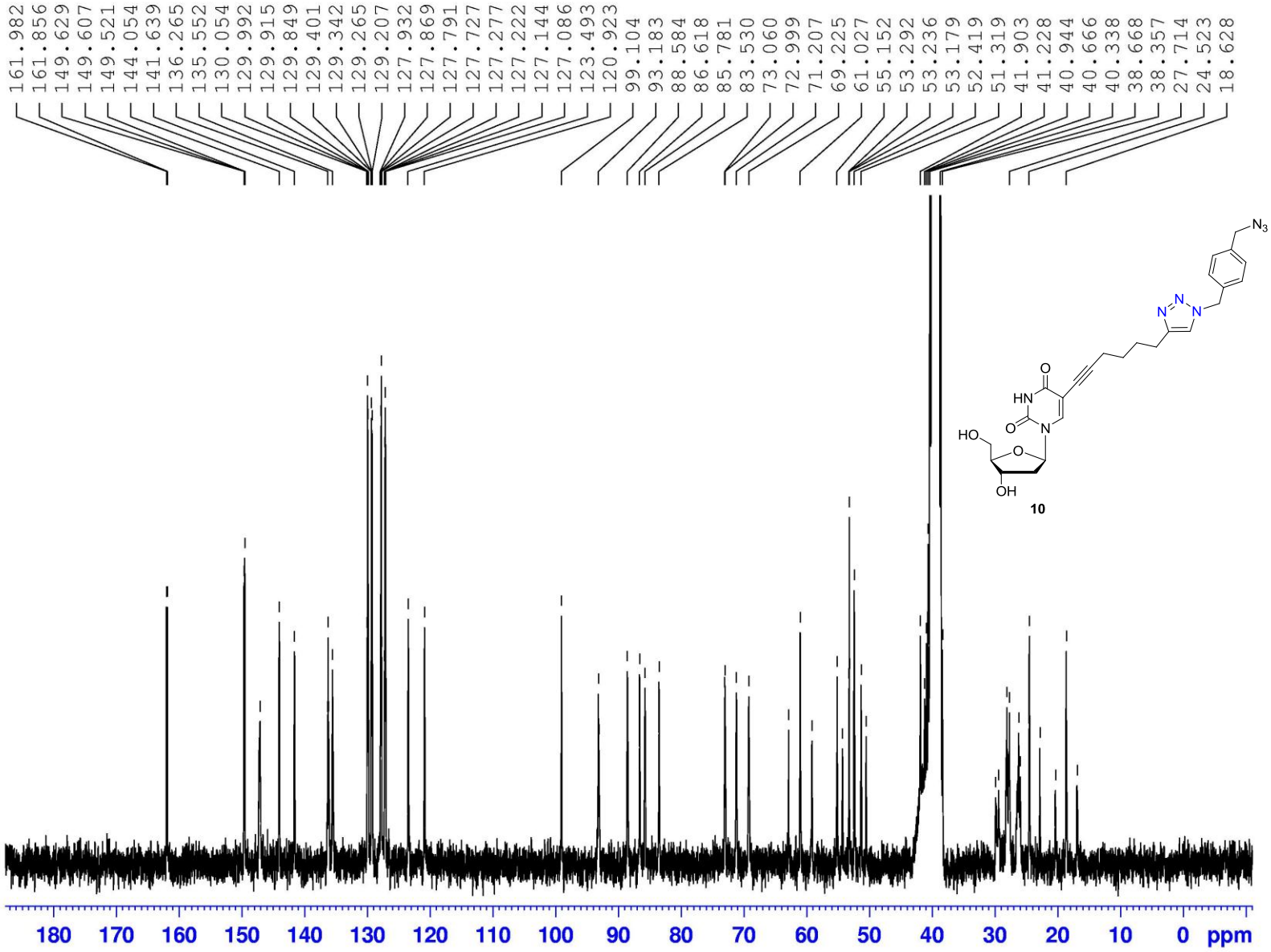

Figure S47. ^{1}H-^{13}C-gated decoupled spectrum of compound **10**.